Journal of Structural Geology 31 (2009) 128–149

Contents lists available at ScienceDirect

Journal of Structural Geology

journal homepage: www.elsevier.com/locate/jsg

Unmasking the 1349 earthquake source (southern Italy): paleoseismological and archaeoseismological indications from the Aquae Iuliae fault

Paolo Antonio Costantino Galli [a,b,*], José Alfredo Naso [a]

[a] Dipartimento della Protezione Civile, Via Vitorchiano 4, 00189 Rome, Italy
[b] CNR – Istituto di Geologia ambientale e Geoingegneria, Via Bolognola 7, 00183 Rome, Italy

ARTICLE INFO

Article history:
Received 2 May 2008
Received in revised form
15 September 2008
Accepted 30 September 2008
Available online 1 November 2008

Keywords:
Active tectonics
Earthquakes
Paleoseismology
Archaeoseismology

ABSTRACT

The 9th September, 1349, earthquake was one of the most catastrophic events experienced along the Apennines. At least three main shocks struck a vast area of the Molise–Latium–Abruzzi regions, and damage was even sustained by the distant monumental buildings of Rome. The southern-most shock (Mw ~ 6.7) occurred at the border between southern Latium and western Molise, razing to the ground the towns of Isernia, Venafro and Cassino, amongst others, and devastating Montecassino Abbey. As with other Medieval catastrophic sequences (e.g., in December 1456, Mw ~ 6.5–7.0), this earthquake has not yet been associated to any seismogenic source; thus, it still represents a thorn in the flesh of earthquake geologists. We have here carried out a reappraisal of the effects of this earthquake, and through an interpretation of aerial photographs and a field survey, we have carried out paleoseismological analyses across a poorly known, ~N130 normal fault that crosses the Molise–Campania border. This structure showed repeated surface ruptures during the late Holocene, the last one of which fits excellently with the 1349 event, both in terms of the dating and the rupture dimension. On the other hand, archaeoseismic analyses have also indicated the faulting of an Augustean aqueduct. The amount of apparent offset of the aqueduct across the fault traces shows that there were other surface faulting event(s) during the Roman–High Middle-Age period. Therefore, in trying to ascertain whether these events were associated with known (potentially of 346 AD or 848 AD), or unknown earthquakes in the area, it became possible that this ~20-km-long fault (here named the Aquae Iuliae fault) is characterized by high slip rates and a short recurrence time. This is in agreement with both the similar behaviour of the neighbouring northern Matese fault system, and with recent GPS analyses showing unexpectedly high extension rates in this area.

1. Introduction

There are many geodynamic secrets hidden amongst the folds of the Apennine chain, and the answers to many questions concerning its seismogenesis remain within its faults. From northern Tuscany to Calabria, the Italian Peninsula has been struck at least sixty times by Mw ≥ 6.0 earthquakes in the past two millennia, half of which were with Mw > 6.5. Although almost all of these earthquakes originated within the upper crust (i.e., from ~15 km in depth) because of the extensional processes currently ongoing along the chain (i.e., $\sigma 3$ ~ perpendicular to the axis), only a few causative faults have been identified to date. In the 1990's, through the awareness that in Italy surface faulting was also a likely occurrence (e.g., in the 1980 Mw 6.9 Irpinia earthquake; Fig. 1), earthquake geology received a large impulse, and several studies on active tectonics and paleoseismology were published. However, whereas our seismotectonics knowledge is today well documented in the Umbria–Abruzzi chain (central Apennines), we still know very little about the seismogenic faults of the northern and southern Apennines. This knowledge gap has a logical explanation for the northern sector, where current strain rates and earthquake magnitudes are lower than for the rest of the Apennine chain; in other words, seismogenic faults are generally below the lower boundary of surface visibility (Mw < 6.5), and thus earthquake geologists have difficulties in the search for their geomorphological signatures. Instead, the southern Apennines are characterized by the strongest and most frequent earthquakes of the chain, while almost all of their causative faults remain unknown. This is also true for the Mw ~ 7 earthquakes, such as those which occurred in Irpinia (1694), Sannio (1688), Basilicata (1857), and for the Medieval seismic sequences of 1349 and 1456 (Fig. 1). Apart from suggestive seismogenic hypotheses derived from geophysical prospecting or from inversion of the

* Corresponding author. fax: +39 06 68202877.
E-mail address: paolo.galli@protezionecivile.it (P.A.C. Galli).

0191-8141/$ – see front matter © 2008 Elsevier Ltd. All rights reserved.
doi:10.1016/j.jsg.2008.09.007

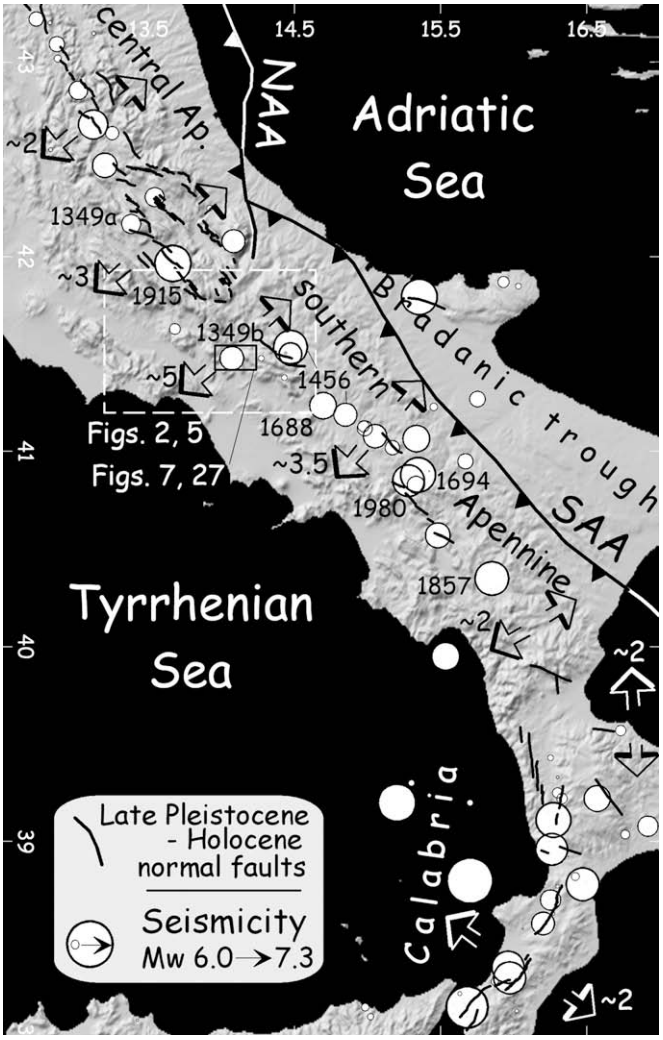

Fig. 1. Seismotectonic sketch of central-southern Italy. NAA and SAA are the northern, and southern Apennine Arcs, respectively. The earthquakes (Mw > 5.9) are modified from Working Group CPTI (2004) (years indicate the events quoted in the text). Faults are from Galli et al. (2008a). Note that almost all the seismicity is elongated along the axis of the Apennine chain. Note also the lack of many active faults in the southern Apennines (i.e., due to our scarce knowledge), with respect to the central ones. Arrows indicate GPS-derived extension rates (values in mm/yr; from Serpelloni et al., 2006; Mantenuto et al., 2007; Mantenuto and D'Agostino, 2007; Giuliani et al., in press).

macroseismic data, these great earthquakes present aspects that need to be resolved.

Here, we attempt to broaden our knowledge of the southernmost main shocks of the 1349 sequence (listed with a Mw of 6.3–7.2 in the different Italian seismic compilations), for which no ideas have arisen concerning its causative fault. After a reappraisal of the earthquake effects, we carried out an aerial-photography interpretation and field survey focusing on a poorly known, ~N130 normal fault that crosses the Molise–Campania border. Thanks to paleoseismological analyses, and archaeoseismic surveys carried out along an unexplored Augustean aqueduct displaced by the fault, we provide valuable information on the recent activity of this structure. Numerical dating, compared with known historical earthquakes of the region, constrains the age of the last events generated by this fault, which we have here called the *Aquae Iuliae fault* (AIF, as below).

On the whole, the data gathered in this study account for the primary role of the AIF in the seismotectonics of the region, both in terms of extension rates and of seismic hazard.

2. Background

2.1. Seismotectonics of the Apennines

The Neogene–Quaternary kinematic evolution of Italy is driven by interactions between the African and Eurasian plates, which are currently converging at a rate ~10 mm/yr along an ~N–S direction (De Mets et al., 1990). This apparently simple framework is greatly complicated by the presence of the Adria microplate, a promontory of Africa towards Eurasia, which causes active compression all along its borders, and the growth of the broad Adria-verging outer (Dinarides; southern Alps) and inner (northern Apennine Arc: NAA; Calabrian Arc) thrust systems.

Conversely, in the southern Apenninic Arc (SAA; Fig. 1), this compression front is no longer active, and has been such at least since the Early-Middle Pleistocene. Therefore, whereas the seismicity from the northern to the eastern borders of Adria (i.e., from the Marche–Abruzzi offshore to the Dinarides–Albanides, going clockwise) is mainly due to thrusting and transpressional faults, the seismicity along the Apennines is due to complex geodynamic mechanisms (e.g. see Pondrelli et al., 2006, and reference therein), that are partly due to the flexure–hinge retreat of the SW-subducting Ionian–Adriatic slab (contemporary to the Tyrrhenian basin opening), and to the postorogenic gravitative collapse of the chain (Malinverno and Ryan, 1986; Royden et al., 1987; Patacca et al., 1990; Doglioni, 1991; Doglioni et al., 1994; D'Agostino et al., 2001). In particular, the axes of the chains of both the NAA, and the SAA are characterized by medium–strong extensional events ($6 < M < 7$; see Working Group CPTI, 2004; CPTI04 from now), which are mainly caused by an NW–SE normal fault system (i.e., a soft-linked array). The faults generally bound intermontane basins (Galadini and Galli, 2000), accounting for a general NE–SW extension of the chain (Montone et al., 2004; Serpelloni et al., 2005), which has recently been quantified by GPS analyses (Fig. 1) as between ~2 mm/yr (Umbrian and Calabrian sector), and ~3–5 mm/yr (Abruzzi and Campania; Serpelloni et al., 2006; Mantenuto and D'Agostino, 2007; Mantenuto et al., 2007; Giuliani et al., in press).

The investigated area falls within the northern sector of the SAA (see inset in Fig. 1). The structure of this first-order-arc is basically a buried duplex system of Mesozoic–Tertiary carbonate thrust sheets, overlain by an up to 9000-m-thick pile of rootless nappes, which derive from platform and basin depositional realms (Patacca and Scandone, 1989; Cinque et al., 1993). Over the last 0.7–0.5 My, it has been affected by NE–SW extension (Ward, 1994), and the largest deformations, strongest earthquakes and evidence of active normal faulting have been seen mainly along the axial belt (e.g. see Galli et al., 2008a, and references therein). Nevertheless, we know very little about most of the faults that were responsible for these earthquakes. Our present knowledge gap and the lack of recognition of seismogenic faults comprise a wide sector of the SAA. Apart from the deep structural complexity of the inherited fold-and-thrust belt chain, the difficulty in identifying active faults is mainly due to the high erodibility of the siliciclastic units that form the surface structure of the seismogenic belt. Under climatic conditions of the late Quaternary, rates of erosion in these rocks preclude the preservation of tectonic surface landforms (e.g., fault scarps) generated by short-term, low-rate (<1 mm/yr) slip rates. Thus, it is not by chance that the only paleoseismic investigations in the southern Apennines have focused on faults affecting erosion-resistant carbonate rocks, as with the N-Matese faults (Blumetti et al., 2000; Galli and Galadini, 2003), the Mount Marzano fault system (Pantosti et al., 1993), and the Caggiano fault (Galli et al., 2006).

As indicated above, an ongoing NE–SW extension in the investigated area is also supported by recent geodetic data. In particular,

continuous GPS measures along an NE–SW transect (1994–2007; see third GPS arrow from the north in Fig. 1. Giuliani et al., in press) have revealed net velocity steps both north and south of the western Matese Massif (see Fig. 2), which account for high regional strain rates (~70 nanostrain/yr). According to Giuliani et al. (in press), the measured strain is consistent with ~4–5 mm/yr NE–SW extension, bipartitoned in the north-eastern (~1.8 mm/yr) and south-eastern (~2.7 mm/yr) flanks of the Matese Massif. These data fit well with the existence of the active N-Matese fault system (Galli and Galadini, 2003; NMFS, in Fig. 2), the slip rate of which is amongst the highest known in the chain (~0.9 mm/yr). On the other hand, the provision of further information as to the other structure(s), which is needed to understand part of the extension on the SW flank of the Matese Massif, is the aim of the present study, and will be discussed in the next sections.

2.2. Seismicity of the investigated area

The seismicity of the Latium–Abruzzi–Molise–Campania border area (see insights in Molin, 1995) is dominated by the catastrophic Middle-Age sequences of September 1349 (see Section 3) and December 1456. Both are characterized by multiple Mw > 6.5 mainshocks which had devastating effects that were spread over entire sectors of the southern-central Apennines. In particular, the 1456 central mainshock (Magri and Molin, 1984; Meletti et al., 1988) occurred in the Bojano basin (Mw 7.0; Fig. 2), and on the basis of a paleoseismological study, it has been tentatively associated to the NMFS (Galli and Galadini, 2003; Fig. 2). According to the latter study, these faults were responsible for two other disruptive earthquakes, one in ~280 BC (unknown to seismological record), and the last one in 1805 (Mw 6.6, Fig. 2; see Galli et al., 2008a). During the first millennium AD, this region was hit by two other strong earthquakes: the so-called 346 AD and 847 AD events. The first of these was quoted by St. Jerome (4th cent. AD) as having occurred during the 281st Olympiad (~348–352 AD), and was dated to 346 AD by Manetti (1457); it has been the object of detailed archaeoseismic studies (Galadini and Galli, 2004) that revealed the occurrence of synchronous destruction of many Roman monumental buildings during the middle 4th century AD, including one case in ~355 AD (Capini and Galli, 2003; Fig. 3).

Whereas paleoseismological analyses exclude the NMFS as the causative structure of the mid 4th century event (Blumetti et al., 2000; Galli and Galadini, 2003), the damage distribution depicted by Galadini and Galli (2004), which is supported by 26 coeval epigraphs, four explicitly attesting to the earthquake[s], and the others to the subsequent restoration), has allowed the epicentre to be placed in the broad southern Matese region (Fig. 2). Nevertheless, this damage, the epigraphs and the historical source might refer to different earthquakes that occurred in the region at the beginning of the second half of the 4th century (some epigraphs quote the plural *terremotibus*), and their effects possibly added to those caused by the earthquake(s) that occurred before 375 AD in the Benevento area (see Symmacus, 4th century AD).

The June 847 earthquake was described briefly by the Chronica Sancti Benedicti Casinensis (9th century; see also Chronica Monasterii Casinensis, 12th century) as striking part of the Benevento Principality (which at that time included part of the present Molise Region), destroying the monastery of San Vincenzo a Volturno, and the town of Isernia. This event was also strongly felt in the distant Rome (Liber Pontificalis, 9th–15th century). According to Guidoboni et al. (1994), who dated this earthquake to 848, the town of Telese was also destroyed. However, this actually happened the year before, and it was due to a Saracen assault (see Figliuolo and Marturano, 2002). Therefore, we do not consider Telese in our tentative placement of the epicentre, which thus falls between Isernia and the San Vincenzo Abbey (Fig. 2).

Other moderate earthquakes have struck this region in past centuries, as in 1654 (Mw 6.2), when heavy damage and casualties were inflicted upon the southern Latium–Abruzzi region (Io 9–10 MCS), and the 1873–1874 earthquakes (Mw 5.4–5.5), which were again at the border between southern Abruzzi and Latium (Io 7–8 MCS). In 1922, an event (Mw 5.6; Io 7 MCS) hits the Sora area. In

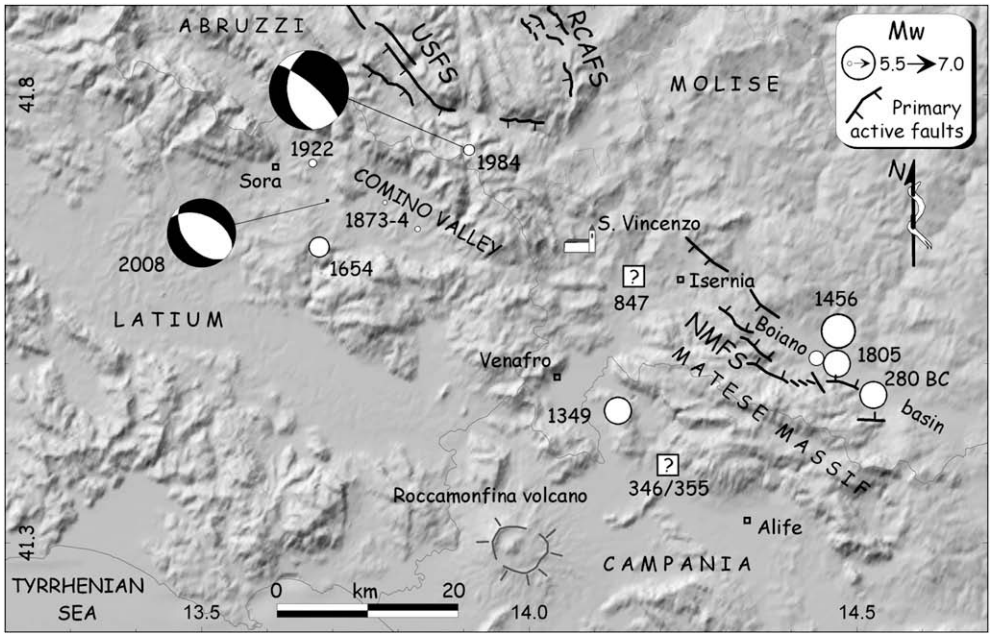

Fig. 2. Shaded relief view of the Latium–Abruzzi–Campania–Molise border area, showing the epicentre of the main earthquakes (Mw > 5.5), and the known primary active faults (teeth on down-thrown side: USFS, Upper Sangro fault system; RCAFS, Mount Rotella–Cinquemiglia–Aremogna Plains fault system; NMFS, northern Matese faults. Modified from Galadini and Galli, 2000). Earthquake epicentres are derived from CPTI04, except: 280 BC (Galli and Galadini, 2003); 346/355 (based on data in Galadini and Galli, 2004); 847 (based on data in Figliuolo and Marturano, 2002); 1349 (this paper); 1984 (in Molin, 1995). Note that almost all of the strongest events cluster NE and SW of the Matese Massif. The two focal mechanisms are the Mw = 5.8, May 5, 1984 event (Anderson and Jakson, 1987), and the Mw = 4.2 event occurred on February 20, 2008 (MedNet, 2008). Both show NE–SW extension driven by NW–SE normal faults.

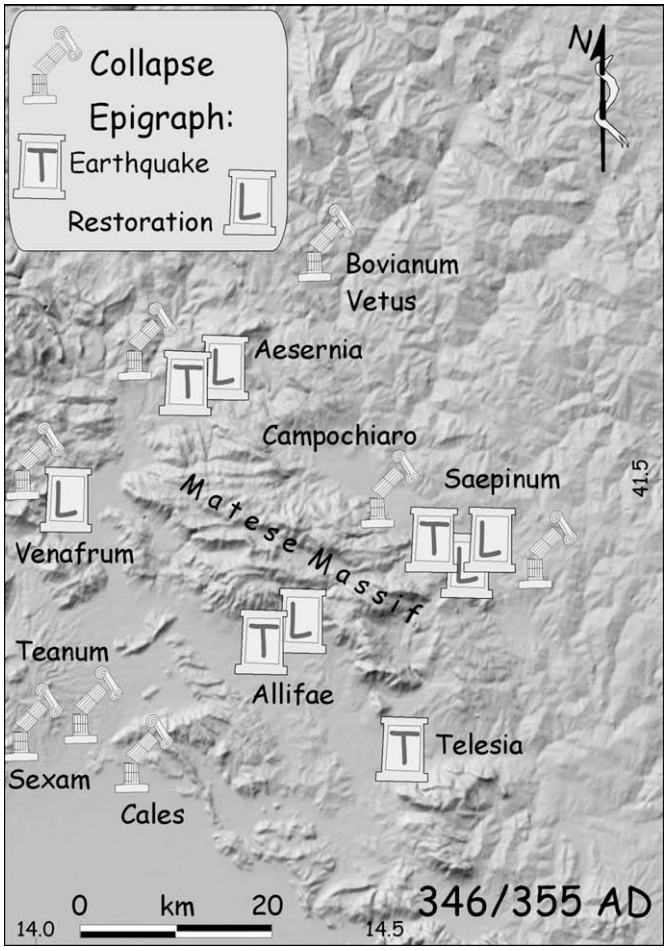

Fig. 3. Distribution of supposed earthquake-induced collapses, and inscriptions related to the 346/355 earthquake(s) (modified from Galadini and Galli, 2004). We cannot definitively attribute all of the indicated effects to only one earthquake. It is reasonable that this picture depicts the damage due to different events cumulated in the area during the 2nd half of the 4th cent. (e.g., the 346/355 earthquake(s), and the ante-375 earthquake).

1984, two strong shocks (Mw 5.8; Io 7-8 MCS) occurred in the mountain areas in Latium, Molise and Abruzzi. For these earthquakes, Westaway et al. (1989) and Pace et al. (2002) have hypothesized a complex rupture of the NNW–SSE Upper Sangro fault system (USFS in Fig. 2; see also main focal mechanism), including E–W segments of the same fault system.

Apart from the uncertainties that accompany the historical determinations of some epicentres (e.g., for those of 346/355, 847), it is possible to see that almost all of the strongest earthquakes of this region have been clustered around the Matese Massif, and as a secondary site, in the broad Comino Valley (see Fig. 2). Nothing more can be deduced from the instrumental seismic catalogue (CSI 1.1, 1981–2002, in Castello et al., 2006), which only notes the 1984 sequence and another low-magnitude sequence near Isernia (1985, Ml 4.1). Finally, on 20 February, 2008, an Mw 4.2 earthquake occurred within this investigated area, on an NW–SE normal fault (with a hypocentral depth of ~10 km). As with the 1984 event, it confirms an ongoing NE–SW extension in the region (see Fig. 2).

3. The 1349 earthquake effects

The effects of the 1349 earthquake cast a vast echo across the Medieval sources, with it being reported and emphasized in many Annals, Chronicles and coeval scripts. It even gained mention in the letters of Petrarch (the famous poet and father of Humanism), where he describes the damage to the monumental buildings of Rome (Petrarch, 1350, 1353; Fig. 4), and strong effects were also in Naples (e.g. in Cronicon Siculum, 14th century). This earthquake also appeared in the early seismic compilations, starting from Manetti (1457) (who gave a date of ~1350) and Pacca (16th century), while Bonito (1691) gave a vivid account of the damaged towns, quoting correctly and documenting many primary sources. A modern view of the earthquake can be found in Baratta (1901), who is the first person to hypothesize the near-contemporary activation of different seismic sources. At the end of the last century, archive researches managed to depict a less vague distribution of the effects (ENEL-ISMES, 1986), with two distinct epicentral areas identified: the first on 9th September (Io 10 MCS; 1349b in Fig. 1) at the southern Latium–western Molise border, and the second on 10th September (Io 9–10 MCS; 1349a, in Fig. 1), near L'Aquila, in the Abruzzi. Nevertheless, the ENEL-ISMES (1986) study does include several misleading pieces of data on localities that were definitely not affected by the earthquake, or were not reported by any of the primary sources, which makes the understanding and parameterization of the different shocks complicated. For example, an intensity of 10 MCS was assigned to Cerreto Sannita, on the basis of news that – in actual fact – refer to the 1688 earthquake; moreover, Boiano (9 MCS), Pescocostanzo (8–9) MCS, and Tocco da Casauria (9 MCS) do not appear in any contemporary sources. These misleading data still survived in Boschi et al. (1995, 1997, 2000), where the seismic sequence is split into three separate epicentral areas (i.e., the L'Aquila region, southern Latium–western Molise, and northern Latium–Umbria). Finally, a new revision of the seismic sequence is in Guidoboni and Comastri (2005), who make a tacit amendment of the previous mistakes, but who also introduce a fourth inexplicable epicentral area (i.e., in the Sulmona region, Abruzzi).

Table 1 summarizes this complex situation, showing the parametric data of the event according to the different seismic catalogues. It is worth noting that the epicentre bounces back and forth from Latium to Molise (e.g., $14^\circ < \text{Long} > 14^\circ$, respectively), while the magnitude calculated from the macroseismic data inversion spans from 6.3 (Guidoboni and Comastri, 2005) to 7.2 (Boschi et al., 2000).

3.1. Reappraisal of the historical sources

Here, we will focus on the southern-most shock, which is the most characterized in terms of the distribution of its effects. We have collected and re-analyzed all of the primary sources that are available, with an evaluation of the site intensity values (Is) for 24 localities using the MCS scale implemented by Molin (2003) (Table 2).

The most damaged villages ($\text{Is} \geq 10$ MCS) were grouped just across the present Latium–Molise border, and included Venafro, Cassino, Cardito, Cerasuolo and, very doubtfully, Atina (Fig. 5). Heavy destruction ($9 \leq \text{Is} \leq 10$ MCS) also affected Alvito, Balsorano, Arpino, Isernia, Sora and Veroli, while the famous Montecassino Abbey suffered heavy damage and collapses. In the mesoseismic area, the most detailed and conclusive coeval information come from Venafro and Cassino (former San Germano). In particular, according to a coeval parchment paper that we can read in Isernia (Anonymous, 14th century; Fig. 6), Venafro was totally destroyed, with 700 casualties (i.e., >10% of the inhabitants at the time: "…*In super destruxit Civitatem Venafri totaliter, et per totum, in qua mortui fuerunt fere homines septingenti, et multa alia, quae difficile esset per totum narrare*…"). Due to the high level of destruction, some quarters of the town were not rebuilt (as can still be seen today), including the cathedral area (see Notar Santo di Venafro, 1423), and the municipality was given a tax dispensation for a long period (see Maria Duracii, 1358; Iohanna Duracii, 1370), together with some neighbouring villages (Ladyslaus Duracii, 1401). In Cassino, half of

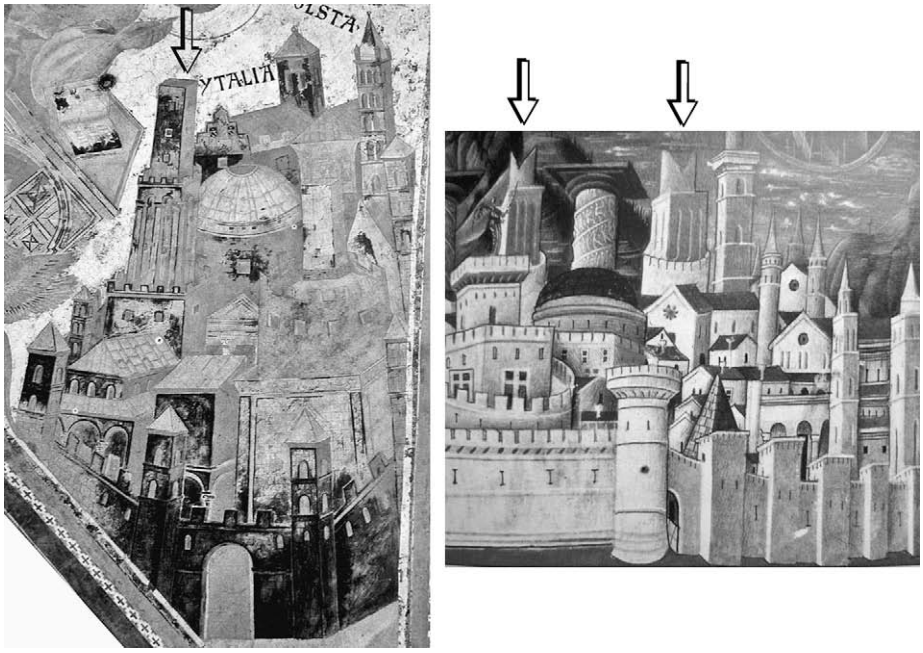

Fig. 4. Left panel: Cimabue's ideal view of Rome (end of the 13th cent. Assisi, basilica of St. Francis). Note the intact Tower Militiae (left of the word Ytalia) that, together with the Conti's one, and with other monumental building of Rome (perhaps, the Coliseum itself), will be heavily damaged by the 1349 earthquakes (Petrarch, 1350, 1353). In the skyline of Rome subsequent to the earthquake, the two towers appear cut-off (e.g., right panel: miniature of Polani (1459). Note the Militiae and Conti's towers at the left and centre, with the damaged top).

the town collapsed, in the zones in the alluvial plain, and many people died ("*…civitas quoque Sancti Germani media corruit precipue illa pars quae erat in plano seu paludibus et in ea innumera multitude hominum ac mulierum mortua est…*"; Anonymous Monachus Casinensis, 13th–14th century).

As far as the effects on other villages of the mesoseismic area are concerned, while the fortresses of Cardito and Cerasuolo are explicitly mentioned in the same parchment of Isernia ("*…Destruxit nihilominus totam provinciam cominus, fortilitia Cardeti, Cerasoli…*"), the information about Atina is not univocal. Indeed, the only known primary source here is the Chronicon breve Atinensis ecclesia (14th century), which says that "it did not stay stone over stone, and many men and women were killed". It is not clear whether this news is generic (as it appears to be), or whether it specifically referred to Atina. The same parchment reported further heavy damage in the town of Isernia itself, and for the monastery of San Vincenzo a Volturno. Finally, in Alvito, the castle and the surrounding village were almost destroyed, as stated by a long-lost epigraph, carefully transcribed by Prudenzio (1574).

3.2. Possible site effects

Apart from the quality and truth of the historical news, which could jeopardize the site intensity evaluation, damage in some of the localities may have been amplified by local geological conditions. Site amplification sometimes distorts the expected shaking distribution, which can be modelled using a defined seismogenic source (e.g., see seismogenetic box in Fig. 5). This is the case for Balsorano, where damage was due to a landslide that involved the castle (Villani, 14th century), as happened again because of the neighbouring 1915 Fucino earthquake (Mw 7.0; see Molin et al., 1999). On the other hand, the Anonymous Monachus Casinensis (13th–14th century) explicitly describes damage in San Germano (Cassino) as only in the part of the town that was in the alluvial plain. In modern earthquakes, these bipartitioning effects are commonly seen for settlements partly built on bedrock and partly on soft sediments (e.g., in Lermo and Chavez-Garcia, 1994; Tertulliani, 2000). The same effects probably occurred in Sora, which shares the same geomorphological condition, as reported by Berardi et al. (1999) for the 1915 earthquake.

Finally, to be certain whether the 1349 destruction in Venafro was not enhanced by local amplification effects, we performed several microtremor analyses (e.g., Galli and Naso, 2008). Our results show no predominant frequency in the range of engineering interest, as expected, considering the local subsoil condition (thick talus debris); therefore, we tentatively exclude amplification phenomena.

As a concluding remark, while noting the highest data-point distribution (Fig. 5) and taking into account possible site amplification cases, the damaged area appears to be NW–SE elongated, but with the strongest effects clustered along its SE edge (i.e., around the Venafro area; Fig. 5). This net elongation might reflect the strike of the source and its related directivity effect (e.g., towards the

Table 1
1349 earthquake parameters in different seismic compilations (southern-most shock). Most catalogues quote the others as the data source, but provide different latitudes, longitudes (and magnitudes), so that the epicentre bounced back and forth from Latium to Molise several times. Magnitude spans from 6.1 to 7.2. Mw/Me, Moment/equivalent magnitude in Gasperini, 2002. Np, number of localities.

Source	Lat	Lon	Imax	Io	Mw	np
PFG85	41.550	13.900	–	0	6.1*	17
ENEL86	41.550	13.900	10–11	10	–	51**
CFT1	41.533	14.050	10	10	7.2	24
CFT2	41.483	14.066	10	10	6.6	24
CFT3	41.483	14.066	10	10	6.7	22
NT96	41.530	13.870	10–11	10	6.7***	49**
CPTI99	41.480	14.070	10	10	6.7	24
CPTI04	41.480	14.070	10	10	6.6	24
G&C05	41.583	13.900	10	10	6.3	20
CFT4	41.583	13.900	10	10	6.8	20
GN08	41.441	14.105	10–11	10	6.6****	24

*, Mk(Karnik); **, cumulated localities; ***, Ms; ****, from empirical relationship fault length/magnitude, in Galli et al., 2008a. Sources: PFG85, Postpischl et al., 1985; ENEL86, ENEL-ISMES, 1986; CFT1-3, Boschi et al., 1995; 1997; 2000; NT96, Camassi and Stucchi, 1996; G&C05, Guidoboni and Comastri, 2005; CFT4, Guidoboni et al., 2007; GN08 introduces the results of this paper.

Table 2
The 1349 earthquake, southernmost mainshock: MCS (Mercalli–Cancani–Sieberg) intensity, evaluated on the basis of coeval sources. D, not estimatable damage. Most of these data points fall in the area of Fig. 5.

Locality	lon	lat	I MCS
Venafro	14.044	41.485	10–11
Atina	13.800	41.619	10
Cardito	13.974	41.590	10
Cassino (San Germano)	13.830	41.488	10
Cerasuolo	14.021	41.584	10
Alvito	13.743	41.689	9–10
Balsorano	13.574	41.800	9–10
Mastrati	14.123	41.406	D
Sesto Campano	14.078	41.420	D
Roccapipirozzi	14.033	41.436	D
Arpino	13.610	41.647	9
Isernia	14.231	41.594	9
Montecassino Abbey	13.814	41.490	9
Sora	13.613	41.718	9
Veroli	13.419	41.692	9
San Vincenzo a Volturno Abbey	14.066	41.633	9
San Domenico monastery	13.579	41.698	8–9
Ausonia (Le Fratte)	13.749	41.354	8
San Vittore nel Lazio	13.931	41.460	8
Sant'Agnello monastery	13.317	41.800	8
Aversa	14.207	40.974	7–8
Naples	14.260	40.855	7–8
Ariano Irpino	15.089	41.153	7
Ascoli Satriano	15.561	41.205	6

NW), as suggested by the seismogenic box obtained by inverting the macroseismic data. (e.g., the Boxer algorithm [Gasperini, 2002] provided a N154° strike: see dashed box in Fig. 2).

3.3. Surface breaks

It is worth noting that apart from landslides, this 1349 earthquake also induced several surficial breaks. The Isernia parchment contains an interesting indication concerning such breaks "caused by the magnitude (*sic*) and power of the earthquakes", and in particular the one that occurred in the Alifae Mountains ("*...fuit tam mira ma[gnitudinis] ac poten[ti]ae, q[uod] mo[n]tes Al[i]fae et plures alios mo[n]tes scidit…*"). At that time, the Diocese of the Alife ruled a vast area of northern Campania, and the southern Matese Mountains were generically named the Alife Mountains (A. Gambella, pers. comm.). Since the Latin verb "*scindere*" ("*montes scidit*") used by the Isernia chronicler means "to cut" (to divide into two, to go across; e.g., scissors), it could have been used to describe a surface faulting phenomena along the hillsides. Therefore, it is possible that surface faulting happened along the southern slopes of the Matese, where it was reasonably accessible/visible from the Volturno Valley (i.e., the route from Venafro to Isernia, or along the ancient *Via Latina*, connecting Venafro to Benevento, via Alife). With this hypothesis in mind, which may now appear weak (i.e., both in paleographic and exegetic terms), we will move on to the next sections.

4. Geology of the investigated area

On the basis of the indications provided by the historical sources (i.e., epicentral area, and location of possible surficial breaks), we focused our preliminary investigation (aerial photograph analyses and field surveys) on the Venafro–SW Matese Mountains. Here we uncovered interesting evidence of recent tectonic activity along an NW–SE normal fault (AIF), the morphotectonic control of which conditioned the Late Quaternary evolution of the landscape. The investigated area can be roughly subdivided into three structural/physiographic units, matching with the Venafro Mountains, the south-western Matese Mountains, and the Venafro Plain–Volturno Valley; the AIF has affected all of these units, raising the NE side of all of them (Fig. 7).

4.1. The Venafro Mountains

These are mainly built up by limestone and dolomite (Upper Cretaceous–Miocene) that has been unconformably layered over

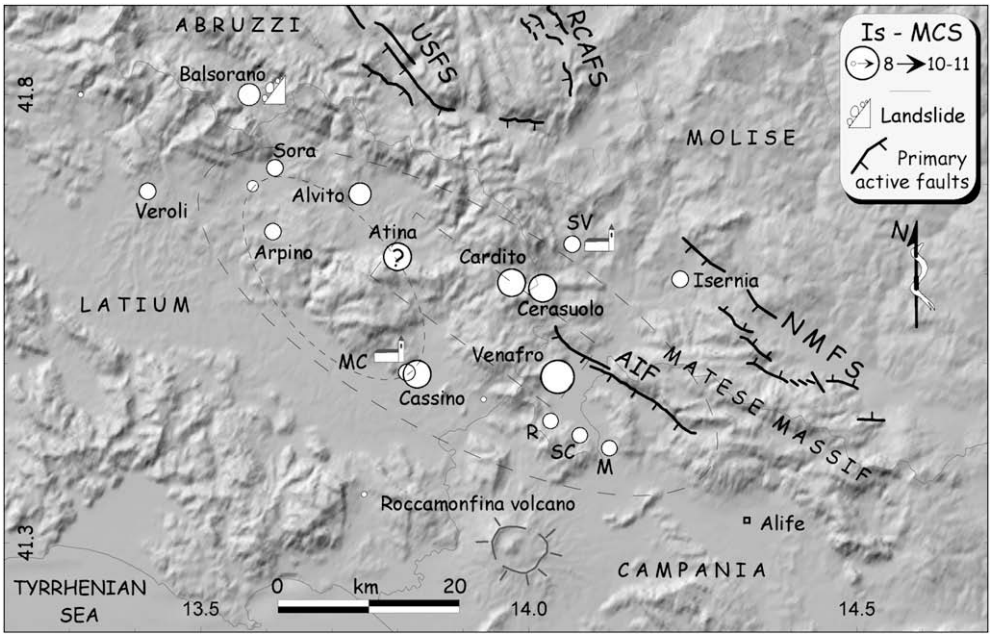

Fig. 5. Shaded relief view of the Latium–Abruzzi–Molise–Campania border, and intensity distribution of the southern 1349 shock re-evaluated on the basis of primary historical sources. Note the net NW–SE elongation of the mesoseismic area (larger dashed ellipse); highest intensity (i.e., the epicentral area) falls in the SE edge, in the Venafro area (Atina is a doubtful point). The dashed box is the seismogenic source inverted by the Boxer algorithm (see text). The smaller dashed ellipse envelops the mesoseismic area of the Mw = 6.2, 1654 earthquake. Primary active normal faults are also shown: USFS, Upper Sangro fault system; RCAFS, Mount Rotella–Cinquemiglia–Aremogna Plains fault system; NMFS, northern Matese fault system (mod. from Galadini and Galli, 2000; Galli and Galadini, 2003). The AIF is also introduced, according to data presented in this paper. R, Roccapipirozzi; SC, Sesto Campano; SV, San Vincenzo a Volturno Abbey; M, Mastrati; MC, Montecassino Abbey.

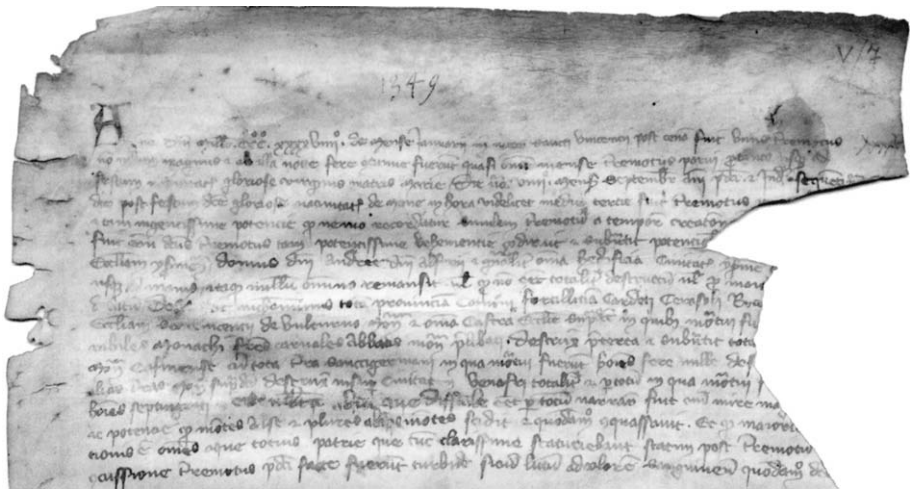

Fig. 6. Isernia parchment paper, recounting the effects of the 1349 earthquake in Isernia, Venafro and other localities. Possible surface faulting phenomena can be inferred from the description of ruptures affecting the hillsides of the area (from Capini and Galli, 2003).

Triassic dolomite and capped by Serravallian marly limestone (SGN, 1971) and Tortonian–Messinian clayey marls (Patacca and Scandone, 2007). In the footwall of the AIF (Fig. 7), N140°–180° marls and marly clays lie unconformably over Lower Miocene limestone (*Briozoi e Litotamni Fm.*), both dipping from ~60° to reversed. The hangingwall is mainly composed of fluvio-lacustrine greyish silty clays and sands, which are at least 80-m thick (local bore–hole data), and which could be reasonably dated to the Middle-Late Pleistocene (Brancaccio et al., 1997, 2000). Further SW, the Rava alluvial fan (Holocene–Present; Otterloo van, 1981) fills the underlying plain, interdigitating its distal portion with the Volturno River deposits. According to bore–hole data, the thickness of the Quaternary succession in the Pozzilli area is 100–120 m (Corniello et al., 1999). Finally, local fans, scree slopes, and colluvia hide vast areas of the hangingwall along the AIF slope (Fig. 8).

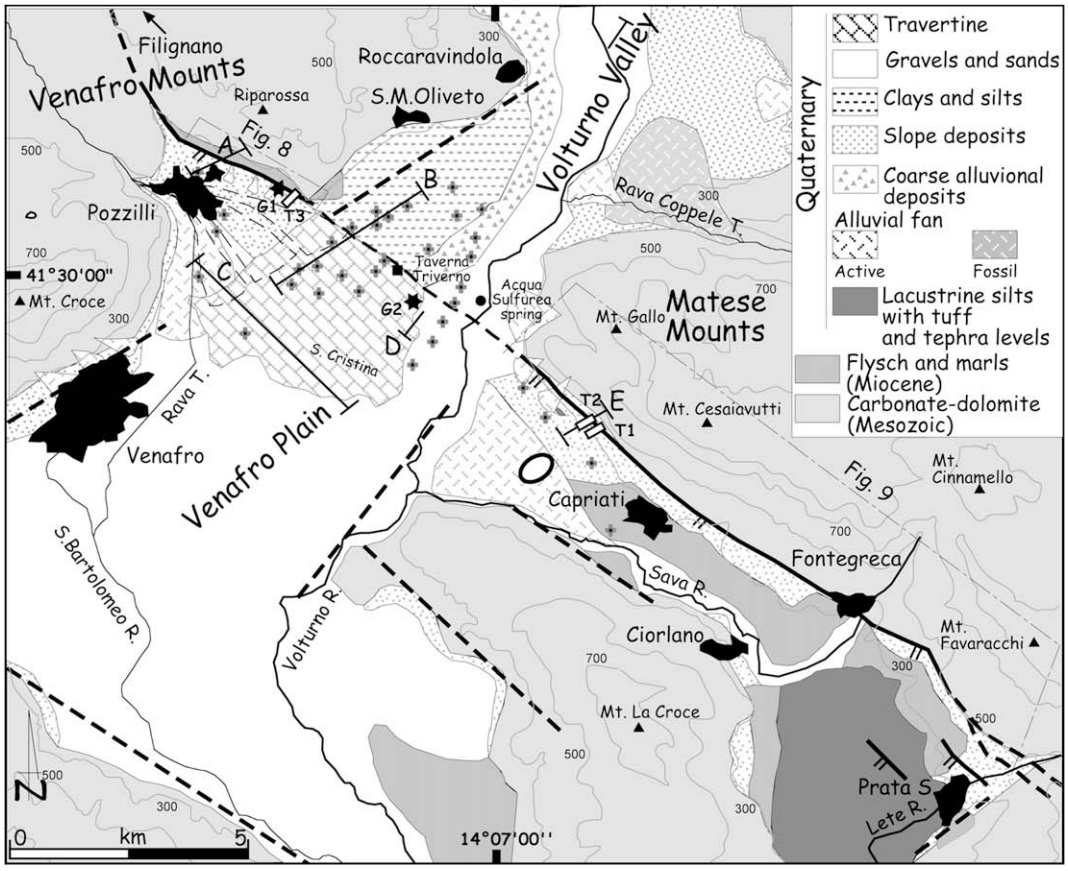

Fig. 7. Simplified geological map of the investigated area, based on data from SGN (1971), Corniello et al. (1999), Otterloo van (1981), and on aerial photograph interpretation and field survey. G1 = geomagnetic survey; G2 = electrical resistivity tomography; T1, T2, T3 = paleoseismological trenches; A, B, C, E = traces of geological sketches; D, fluvial terraces profile; cross symbols indicate bore-holes. Bold line is the Aquae Iuliae fault; dashed lines, inferred and/or buried faults.

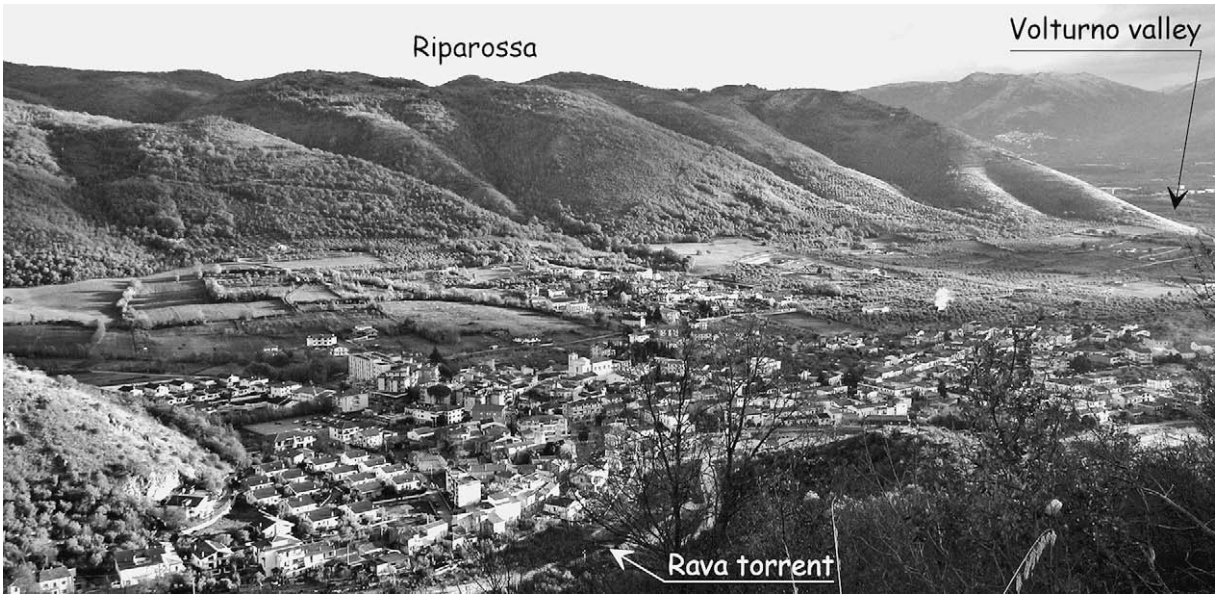

Fig. 8. View looking NE of the Riparossa slope (note Pozzilli in foreground). The visible slope break fits mainly with the Miocene limestone–marls passage, whereas the AIF runs farther downhill, separating the argillitic member of the Miocene formation from the clayey Pleistocene deposits of the hangingwall, without evident surface indication. We were obliged to dig several pits in the field to individuate the fault location. This area has been intensively and continuatively ploughed and cultivated, at least since the Roman times; therefore, any surface fault indication has been easily erased and levelled.

4.2. The south-western Matese Mountains

This sector is characterized by a thick carbonate–dolomite succession (Trias–Miocene) that contains several depositional hiatuses. In the Capriati–Fontegreca area, the Cretaceous limestone lies unconformably over Triassic–Liassic dolomite (SGN, 1971), and it is faulted against Late Miocene flyschoid terrigenous deposits. These last crop out all along the Mount Cesavaiutti slope, starting from Prata Sannita, going towards the north-west (SGN, 1971; Corniello et al., 1999; Fig. 9). Large parts of the paleobasin developed in the hangingwall side of the AIF are filled by terraced lacustrine grayish silts and sands, which contain several tephra levels. According to Bosi (1994), the age of these deposits could be tentatively fixed at around 317–230 ka, which is the age of the White Trachitic Tuff unit (WTT; Giannetti and De Casa, 2000) of the Roccamonfina Volcano. A thick colluvial–eluvial covering, together with fan deposits and scree slopes, mask vast sectors of the terrigenous succession, and of the lacustrine deposits in the down-thrown block of the AIF. In particular, we found rich in tephra deposits (WTT?) along the Mount Cesavaiutti slope (e.g., close to the Volturno Valley; Fig. 7) that have been buried and preserved by a local fan.

4.3. The Venafro Plain and Volturno Valley

Between the Venafro and Matese Mountains, south of the AIF, the Volturno Valley opens into a wide trapezoidal plain (the Venafro Plain). The valley and the plain have different geomorphological arrangements: the valley presents a flight of well-preserved fluvial terraces, deeply carved by the stream network, whereas the plain appears to have been largely over-flooded, and not cut into by the Volturno River or its tributaries. The over-flooding process is still active today, as testified by the elevation of the *arena* of the Venafro Roman Amphitheatre, which we found buried under ~4 m of alluvial and tephra levels, below the water table. Bore–hole data show that the plain and the valley have different sedimentary fillings. The plain has a ~300-m-deep lacustrine succession, interdigitated by slopes and alluvial fan deposits (Lower-Late Pleistocene; Brancaccio et al., 1997). Conversely, the valley is mainly filled with fluvial units (starting from Middle Pleistocene; "*Unità Principale*", *sensu* Coltorti, 1983; Coltorti and Cremaschi, 1981), which are rich in tephra layers (partly coming from the Roccamonfina volcano, and partly from recent Campanian eruptions; Galli et al., 2008c) and can reach 50 m in thickness (Brancaccio et al., 2000).

Fig. 9. View looking SE of the Cesavaiutti–Favaracchi range. The AIF runs at the base of the slope, mainly between the bedrock and the slope deposits. Near Fontegreca the fault separates the Mesozoic rocks from Miocene flyschoid units.

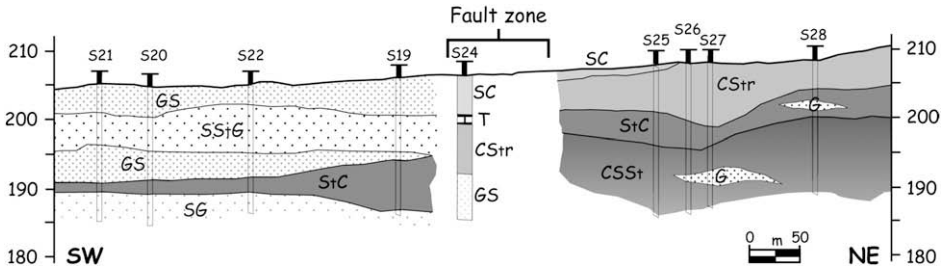

Fig. 10. Sketch across the fault zone along the Volturno Valley (trace B in Fig. 7). According to bore–hole stratigraphy, the footwall and hangingwall show two different depositional successions (mainly gravel and sand the former, *vs* silt and clay the latter). Bore–hole S24 falls in the fault zone, and shows the reddish (r), oxidized silty clays (see CStr in the footwall) lowered by ~10 m. G, gravel; S, sand; St, silt; C, clay; T, travertine.

By means of dozens of bore–hole logs stored at different organizations and institutions, we tried to work out the stratigraphic/tectonic relationships between the two successions. Due to the strong lateral and vertical variation of the fluvio-lacustrine and fan deposits, it was actually very difficult to correlate single depositional bodies along a section; however, Fig. 10 highlights the general lithological difference between the NE and the SW sectors. That NE is characterized by fine sediments, as mainly clays and silts, while in the SW sector, coarse deposits prevail (i.e., gravels and sands of the distal portion of the paleo-Rava alluvial fan). Moreover, the only level which appears to be correlative at the top of both successions (reddish, oxidized silty clays, gently dipping towards SW; CStr in Fig. 10) deepens abruptly ~10 m across the AIF zone, and then disappears.

4.3.1. Travertine

SW of the AIF traces, a travertine plate crops out (Fig. 7), which is capped by a ~1-m-thick calcic cambisol. In plan, it has a rough trapezoidal shape (~4 km^2), which is limited on its NW side by the Rava di Pozzilli fan, and by the Volturno basal plain on its SE side. The travertine is mainly of phytohermal origin, and contains much leaf mould, frustules and other parts of plants. The phytohermal facies is characterized by the presence of lenticular intercalation (i.e., pool infilling) of calcareous sands and colluvia, and by a ~1-m-thick yellowish tephra (Fig. 11). This last is characterized by a repetition of centimetre-thick fine and coarse ash layers, which is mainly well-vesiculated micro-pumice and platy glass shards, with sparse feldspar crystals (see microprobe chemical analyses performed on handpicked fresh glass shards in Table 3, Venafro CEM sample). Both its stratigraphic features and its variable composition (from latite to trachyte–phonolite) strictly replicate those of the Neapolitan Yellow Tuff (i.e., the product of the second largest eruption from Campo Flegrei caldera; Orsi et al., 1992) dated 14.9 ± 0.4 ka BP (Deino et al., 2004).

In some places, lithoid travertine forms the outer border of flat depressions that have been filled by detritic travertine and alluvial/colluvial deposits (with Neolithic, Roman and Middle-Age relics; Otterloo van, 1981), and have sometimes been cut into by erratic streams that arose from the Rava fan. The thickness of the outcropping plate can reach 1–3 m; however, bore–hole data show the presence of at least another >4-m-thick level ~10 m below the ground surface. This fits with the results of geoelectrical analyses (using electrical resistivity tomography) that we performed at the eastern border of the plate (site G2 in Fig. 7). Below a first surficial high resistivity body (which correlates with travertine outcrops), there is a second ~4-m-thick level 7 m under the ground surface. According to the tephra levels and to the prehistoric and historical relics, the age of the travertine formation is definitely post-Last Glacial Maximum (LGM).

4.3.2. Terraces

As indicated above, the Quaternary succession outcropping in the footwall is deeply cut by the Volturno River and its tributary, showing a flight of fluvial terraces (Fig. 12; Otterloo and Sevink, 1983; Brancaccio et al., 1997, 2000). Along the high Volturno Valley, we mapped (at least) six different orders of terraces: the highest at ~320 m a.s.l. (i.e., 70 m above the corresponding active alluvial plain), the last one being currently forming. In the investigated area, we found remnants of a 3rd order surface at around 250 m a.s.l. along both sides of the Volturno Valley, dipping slightly down-stream (i.e., 1st order in Brancaccio et al., 2000). On the left bank, its edge cuts the distal portion of the Rava delle Coppelle paleofan, which in turn deeply cut pedogenized silty–sandy deposits (i.e., "*Unità Principale*"). A younger depositional fluvial terrace (4rd order), capped by well developed vertic luvisoil, can be easily followed from ~240 m to 210 m a.s.l., going down-stream on both sides of the valley. In the investigated area, its top always comprises alternating gravels and silty–sandy deposits, containing altered tephra layers. The 5th order surface is visible close to the fault intersection, at an elevation between ~202-193 m a.s.l., linked to a depositional terrace and capped by luvisoil and calcic cambisoil. All these terraces "disappear" crossing the AIF traces, as shown by the profile in Fig. 13 (left bank), whereas the 4th and the 5th seem to be confined by the travertine plate (Galli et al., 2008c).

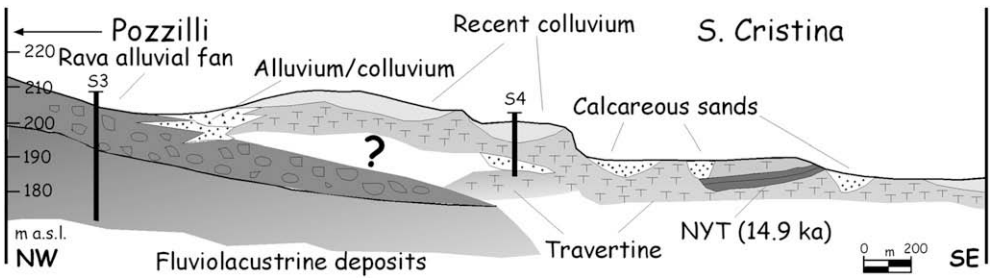

Fig. 11. Sketch across the travertine plate (C in Fig. 7), showing the stratigraphical relationships amongst the different Late Pleistocene units of the area (vertical exaggeration × 10). The tephra level has been identified with the Neapolitan Yellow Tuff (~15 ka; see Tab. 3: B. Giaccio, pers. com.). Mod. after Otterloo van (1981), according to bore–hole data, geoelectrical tomography (ERT), and field survey.

Table 3
Comparative chemical data (WDS-EDS analyses; wt.% normalized to 100%) of the tephra layers sampled in the Venafro travertine, and TM-8 layer of the Monticchio sequence (southern Italy), corresponding to the Neapolitan Yellow Tuff (NYT). a – Wulf et al. (2004); n: number of analyzed shards; sd: standard deviation.

Tephra	Venafro CEM						Monticchio TM-8 (NYT)[a]			
Population	*a*		*b*		*c*		*a*		*b*	
	$n=4$	sd	$n=12$	sd	$n=3$	sd	$n=5$	sd	$n=4$	sd
SiO_2	56.62	1.07	60.29	0.54	61.71	0.42	56.77	0.24	61.66	0.11
TiO_2	0.66	0.04	0.43	0.05	0.43	0.06	0.60	0.03	0.43	0.03
Al_2O_3	18.89	0.03	18.97	0.23	18.81	0.23	18.51	0.08	18.35	0.08
FeO	5.54	0.50	3.51	0.36	2.84	0.26	5.32	0.09	2.87	0.07
MnO	0.13	0.05	0.13	0.06	0.15	0.03	0.14	0.02	0.15	0.04
MgO	1.83	0.36	0.74	0.13	0.46	0.03	1.63	0.07	0.44	0.03
CaO	4.92	0.57	2.68	0.29	2.12	0.04	4.83	0.15	2.18	0.03
Na_2O	3.05	0.22	3.57	0.31	4.17	0.35	3.50	0.07	4.91	0.01
K_2O	7.53	0.37	9.04	0.43	8.72	0.64	8.00	0.07	8.49	0.08
P_2O_5	0.37	0.11	0.11	0.04	0.05	0,01	0.36	0.06	0.05	0.03
F	0.11	0.05	0.18	0.10	0.24	0.09	0.00	0.00	0.00	0.00
Cl	0.44	0.05	0.50	0.08	0.60	0.03	0.44	0.02	0.62	0.01
SO_3	0.15	0.09	0.12	0.07	0.02	0.03				
Original total	97.70	0.51	97.54	0.79	98.02	1.81				

The minimum age of the terraces can be inferred by the age of the units in which they are carved or that they top. As far as the 3rd order is concerned, its age is younger that the paleofan of Rava delle Coppelle. We noted that this fan is separated from the "*Unità Principale*" by an important erosional surface and by a thick, evolute paleosol: therefore, on the basis of ^{39}Ar-^{40}Ar dating on volcanic material contained in this unit (Di Bucci et al., 2005), the 2nd and 3rd orders are much younger than 253 ± 22 ka at least (weighted average age of the youngest component of the samples). As far as the 4th order age is concerned, due to the alteration affecting the tephra levels, we are not able to provide correlations with the parent pyroclastic unit. However, the top-surface of this terrace is interfingered with an alluvian fan, that in turn has been dated 14,650–13,800 ka BP (2σ cal.; Galli et al., 2008c). Therefore, the 4th order terrace certainly formed during the end of the Late Pleistocene.

5. The Aquae Iuliae fault

The existence of a fault that partly matched with the AIF was first hypothesized by Otterloo and Sevink (1983: the Pozzilli–Capriati line), who revealed the different distributions of the Volturno terraces north and south of it. Brancaccio et al. (1997, 2000) then suggested a Middle Pleistocene fault activity, whereas, on the basis of the same data, Cinque et al. (2000) indicated a Middle Pleistocene–Holocene timing, with a slip rate of 0.2–0.4 mm/yr.

Aerial photograph interpretation and step-by-step field surveys along the fault traces have allowed us to map it at a 1:5,000 scale, starting from the Filignano area (NW tip), heading to the Prata Sannita area (SE tip), for a length of approximately 22 km (Fig. 7). As we describe below, the fault also cuts an Augustean aqueduct (1st century BC) that brought the imperial waters (i.e., Aquae Iuliae) from the Volturno springs to Venafro. Therefore, we have called this

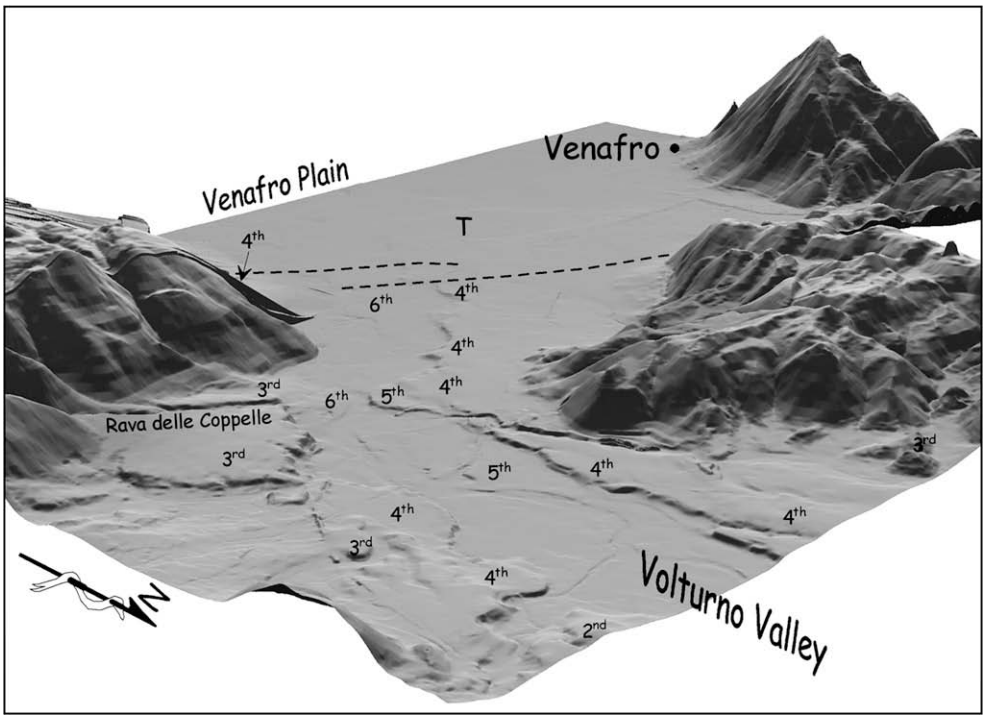

Fig. 12. Three-dimensional view from NE of the Volturno Valley and Venafro Plain (DEM from 1:5000 maps). Note both the flight of different fluvial terraces which disappears crossing the AIF (dashed lines), and the flat, over-flooded Venafro Plain. T is the travertine plate growth in the hangingwall (see Fig. 7).

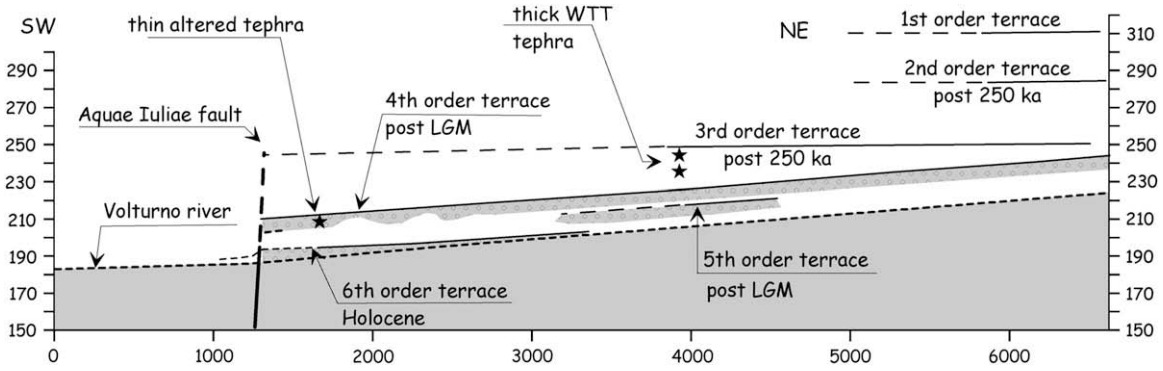

Fig. 13. Terraces profile along the left bank of the Volturno River in the investigated area (elevations are from 1:5,000 maps; trace D in Fig. 7). Note the lack of all the terraces in the hangingwall (simple lines are degradational terraces; hatches, depositional terrace). WTT is the Roccamonfina volcano White Trachitic Tuff (see text).

the "Aquae Iuliae fault", as the Pozzilli–Capriati lineament represents only a part of this longer structure. The fault has an average N125° trend, with N150° strands in the segment north of Volturno Valley (the Riparossa slope), and N115° in the southern segment (the Cesavaiutti–Favaracchi range). It appears on aerial photographs as a net scarp at the base of the Cesavaiutti–Favaracchi range (southern segment), whereas there are only faint indications of its presence in the Riparossa slope (northern segment).

5.1. The Northern segment

In this strand of the structure, the main topographic break does not fit with the fault traces, but with the stratigraphic limit between the Miocene limestone and the marls, which almost parallels the fault (~N140°; Figs. 8 and 14). Therefore, the iron-flats that characterize the entire hillside look as though they are due to the converging activity of the AIF and the morpho-selective processes. On the other hand, the fault traces are indicated only by sparse ~NW–SE smoothed scarps and by the different soil tonality in recently ploughed fields (i.e., light marly soils *vs.* dark colluvia). Going NW, the fault plane rotates clockwise; here we measured the obliquely striated (pitch ~45°) rock-fault plane (left-hand striae), carved inside the carbonate Miocene bedrock.

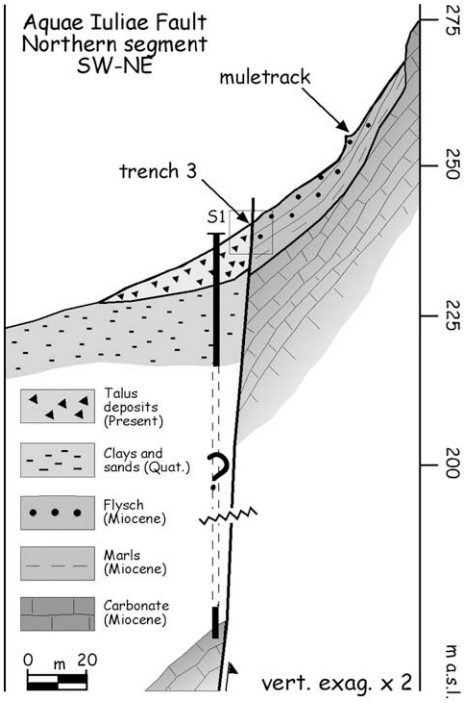

Fig. 14. Geological section across the northern segment of the AIF (trace A in Fig. 7). The main scarp along the slope is controlled by the subvertical limestones–marls passage, whereas the fault does not show any prominent morphological evidence. S1, bore–hole reaching the carbonate basement.

5.2. The Southern segment

The southern segment showed the best faulting evidence. At the base of the lushly forested slopes of Mount Cesavaiutti (Fig. 9), there were several signs of rock-fault-plane outcrop (i.e., *nastro* = ribbon, in the Italian literature; Fig. 15), with well-preserved dip–slip striae (the Capriati–Fontegreca strand). In other places (e.g., north of Capriati and south of Fontegreca) a prominent ~3-m-high scarp is carved into dolomite flour, with rare, badly preserved rock-fault-planes.

Although the fault generally separates the carbonate–dolomite bedrock from scree slopes, in some place it cuts across the slightly cemented slope deposits, which mantled the footwall of the hillside after/during the LGM (~25–18 ka BP). In these cases, an impressive, polyphasic, ~3-m-high free-face that is carved into stratified gravels interrupts the slope profile, forming the base of the retreating fault scarp. At the extreme SE tip of the fault (the Mount Favaracchi slopes), the main fault plane is split into several secondary splays, which cut across the Jurassic limestone. These splays produce mesoscale domino structures, which are not matched by prominent fault scarps.

Fig. 15. Rock-fault plane in the Triassic dolomite. The so-called "*nastro*" can be followed for a hundred metres along the slope between Capriati and Fontegreca, with heights of 2–4 m. Dip–slip striae indicate the main kinematics of the fault. In the hangingwall, below reworked colluvial wedge deposits, we observed the argillitic portion of the underlying flysch deposit.

In the hangingwall of Prata Sannita, and far for the main fault scarp, we noted diffuse N140° faults in the tuff and lacustrine deposits, which displace these units by several metres. Although these deformations do not show evidence of recent motion (i.e., they are not associated with any fresh scarp), they testify to the onset of the NE–SW extension in this area after the deposition of the lake deposit (250 ka), as indicated by Bosi (1994), Brancaccio et al. (1997) and Caiazzo et al. (2001).

5.3. The Volturno Valley

The river floods obviously eroded and covered the fault traces in the Holocene alluvial plain of the Volturno Valley. Conversely, and as previously shown, the 3rd–4th order fluvial terraces, which are several metres above the current Volturno basal level, plunge abruptly down-stream, disappearing across the fault traces (Figs. 12–13). On the right bank of the river, the top of the 4th order surface is progressively covered by colluvial and alluvial deposits that flatten out the present topography, forming a unique smooth surface that also extends onto the travertine plate and onto the Rava fan (Fig. 12; i.e., is the travertine plate that dams the 4th terrace).

Despite this, it is the existence itself of the travertine plate and the thermal springs that might offer further indication about the location of the AIF in the Volturno Valley segment. Indeed, if we assume that the travertine forms due to CO_2 degassing of deeply circulated waters rising along the fractured AIF zone (i.e., carbonate-rich hot waters, as testified by the neighbouring *Acqua Sulfurea* spring, which have been exploited since the Roman period; see Pliny the Elder, 1st century), and eventually mixing with the surface and ground waters of the regional carbonate aquifer, their NE edge could roughly indicate the fault traces at depth (see similar case histories in Altunen and Hancock, 1993; Çakir, 1999; Hancock et al., 2000). This hypothesis actually fits with the field and bore–hole data, showing that the travertine ends NE of the supposed fault traces (Figs. 7 and 12; see also SGN, 1971). Indeed, gas chromatography and mass spectrometry analyses carried out on the gas of the Acque Sulfuree spring (Paternoster, 1999) showed high CO_2 levels, and a $^4He/^{20}Ne$ ratio much greater than that of the atmosphere. On the other hand, the helium isotope ratio ($^3He/^4He$) indicates a net deep crustal provenience of the gas, with a level of mantle degassing contribution (Table 4).

This offers a further indication of the existence of an active fault zone that allows the raising of deep crustal elements. Moreover, we have some indication that in the Volturno valley, the two main AIF segments are not yet completely linked (at least in their upper part), presenting an *en-echelon* geometry. This kind of tectonic arrangement (i.e., relay–ramp zone) results in a complex morphological response in the overlap zone, where the down-thrown block of one fault becomes the raised one of the other, with throws and tilting tapering obliquely at the tips of the two segments (i.e., warping can occur at the fault tip instead of faulting). This is the situation in the Taverna Triverno area (Fig. 7), where after plunging down-stream, the 4th order terrace edge appears again after the Triverno stream, and then disappears below the Holocene plain.

Table 4
Selected data from gas chromatography and mass spectrometry analyses carried out on the Acqua Sulfurea spring (Paternoster, 1999). These results testify to a deep crustal origin of the gas (10% mantle contribution) raising along the AIF ($R = {}^3He/{}^4He$; Ra, Air isotopic ratio $= 1.4*10^{-6}$; c, atmospheric contamination correction).

T° C	Dissolved Ions	CO_2%	$^4He/^{20}Ne$	R/Ra c
20	Ca, Mg (carbonate rocks) Na, Cl, SO_4 (not carbonate rocks)	94–98	48	0.70 Ra (10% mantle contribution)

Moreover, it is known that hydrothermal outflow often occurs at the tip of interacting faults, where high levels of stress cause active fracturing (break-down regions, sensu Scholz et al., 1993) and opening of fluid-flow conduits (see Curewitz and Karson, 1997; Çakir, 1999). Therefore, the thermal springs and the travertine deposition in the Taverna Triverno area could actually indicate the presence of a fault-linkage zone.

6. Paleoseismological analyses along the Aquae Iuliae fault

To obtain analytic data on the recent activity of the AIF, and to determine whether and when it ruptured during historical times, we designed and dug three paleoseismological trenches: two across the Mount Cesavaiutti segment (trenches 1, 2 in Fig. 7), and a third across the Riparossa segment (trench 3 in Fig. 7). Trenches 1 and 2 provided reliable information as far as fault ruptures in the past two millennia are concerned. Conversely, due to a lack of datable material, trench 3 provided data that mainly concerned the fault geometry along the smoothed clayey slopes facing Pozzilli. We had decided to open trenches 1 and 2 at the foot of the Mount Cesavaiutti slope, across the free-face carved in slope deposits, as we hoped to find buried paleosol, and/or to carry out ^{14}C dating of suitable deposits. Here, moreover, the fault affects entirely post-LGM gravel, avoiding complex and scarcely useful excavations across the carbonate footwall.

The local geological framework of these trenches is summarized in Fig. 16, which has been drawn on the basis of 1:5,000 topographic maps, the microtopographic survey (inset A), and the geological field survey. The section reveals the presence of stratified slope gravels that smooth the slope profile, and that join the rocky dolomite hillside with the smooth flyschoid downhill. It is commonly accepted that in the Apennines the deposition of these deposits and the slope smoothing process occurred during the cold and arid climatic phase at the end of the LGM (Dramis, 1983). This has been verified by means of several ^{14}C datings, in both the central and the southern Apennines (i.e., between 20 and 16 ka; Galadini and Galli, 2000; Galli et al., 2006). Therefore, the topographic break that is visible in Fig. 18A ($\sim$4 m) and which is due to repeated fault ruptures and to the subsequent fault scarp retreat, can be reasonably assigned to post $\sim$18 ka faulting, as shown in the next paragraphs.

Further down-hill, the section shows lacustrine silts containing tephra, which are gently tilted counter-mount. They crop out roughly at the same elevation as the analogous Prata Sannita deposits, overlaying the Miocene rocks.

6.1. Trench 1

Due to the impossibility of taking a backhoe to this site (it is a steep and forested area), this trench was hand-dug by a team of specialized workers. Even if it is just 3 m long and 2 m deep, it shows the very detailed stratigraphy of the fault zone. All of the recognized units of the hangingwall are faulted against the slope gravels of the footwall, except for the two upper-most levels (1–2 in Figs. 17 and 18), which seal the fault, burying also part of the retreated fault scarp. Several secondary fault-planes affect the hangingwall deposits, while a decimetric fault damage zone has developed in the footwall. The units in the down-thrown block are mainly colluvial gravel in a sandy matrix, and are faintly stratified with dark silty levels, which breaks represent during the coarse slope deposition. As indicated above, units 8–3 are all faulted against unit 10, with "event horizon 2" (EH2 in Fig. 17; i.e., ground surface at the last rupture) being placed under unit 2. A previous event (EH1) appears to have affected units 8–6, with them being sealed by unit 5. The amount of the offset per-event is not directly measurable here, due to a lack of correlative units across the fault.

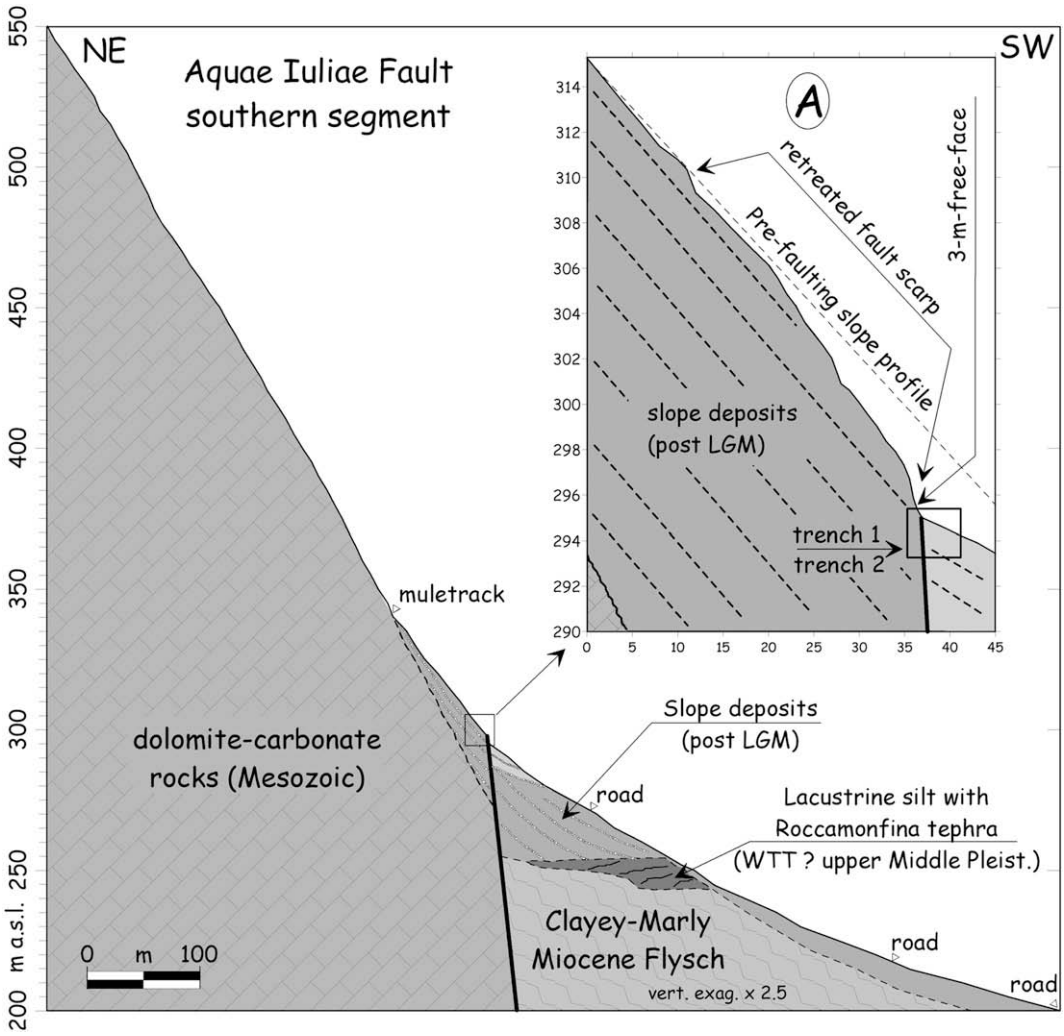

Fig. 16. Geological section along the Mount Cesavaiutti slope (vertical exaggeration × 2.5; section E in Fig. 7). Trenches 1 and 2 were dug into well-stratified slope gravels, at the base of the fault scarp that interrupts the post-LGM rectilinear slope profile (see inset A).

However, by restoring the faulted units, and taking into account the height of the fault scarp, the last rupture was not less than 0.7 m. The offset across the secondary splays affecting units 8–6 reaches, in turn, 0.6 m, which is a minimum value for the previous surface faulting event.

As far as the dating of the succession is concerned, we did not find any relevant charcoal or wood fragments. Therefore, we used low-carbon bulk material, which needed accelerator mass spectrometry processing (Table 5). These samples provided ages that fall into the first half of the last millennium (Low-Middle Age), and according to Fig. 18, there is no doubt that the last rupture occurred during the incipient pedogenization of unit 4 (i.e., unit 3), the time of which falls between 1290 and 1420 AD. This event is sealed by unit 2, dated from 1450 to 1650 AD. The previous event occurred at EH1, which was at an unknown time before 1020–1210 AD (i.e., the top of unit 6 is erosive).

6.2. Trench 2

This trench is located NW of trench 1, in the same geological context. It was also excavated by hand, to a length of 4 m and a depth of 2 m. The footwall shows the same succession as for trench 1 (unit 10), whereas the deposits of the hangingwall differ slightly from those previously described, probably because of the vicinity of a stream. Locally, the fault strikes N160° (it was N145° in trench 1), presenting a 0.5 m thick cataclastic zone that is made up of a cemented damage zone in the footwall and a "lithon" of destructured material that was dragged along the fault plane (unit 9 in Fig. 19). Units 7–3 are mainly colluvial gravels, from massive (unit 7) to well stratified (unit 4), with sandy–silty brownish levels (unit 6 and, partly, 3); they are all faulted against unit 10, and sealed by units 2–1, as in trench 1. In particular, unit 2 (and unit 1, which is its upper pedogenized level, i.e., the present soil) is a gravelly colluvial unit that is partly made up of clasts that have eroded from unit 10; it has a whitish powdered sandy matrix that has derived from the degradation of the cement of the fault plane/damage zone. We found sparse tile fragments within this unit, which can be related to a modern age (L. Scaroina, pers. comm.).

It appears that the last observable rupture in this trench occurred at the top of unit 3 (EH2), which was also dragged along the fault plane. The newly formed fault step was then quickly eroded, with unit 2 being the product of colluviation at the base of the fault scarp. Due to faulting and deposition of unit 2, the incipient pedogenization of unit 3 was also aborted, while the retreated fault scarp was progressively buried by unit 1. A previous event (or more than one) is testified by the faulting of units 7–4 against unit 8, which was sealed by the colluvial deposits of unit 3 (EH1).

Due to the lack of correlative horizons, the offset per-event is not precisely quantifiable; however, we have calculated a minimum of 0.8 m for the last event, and a minimum cumulated 1.5 m offset for

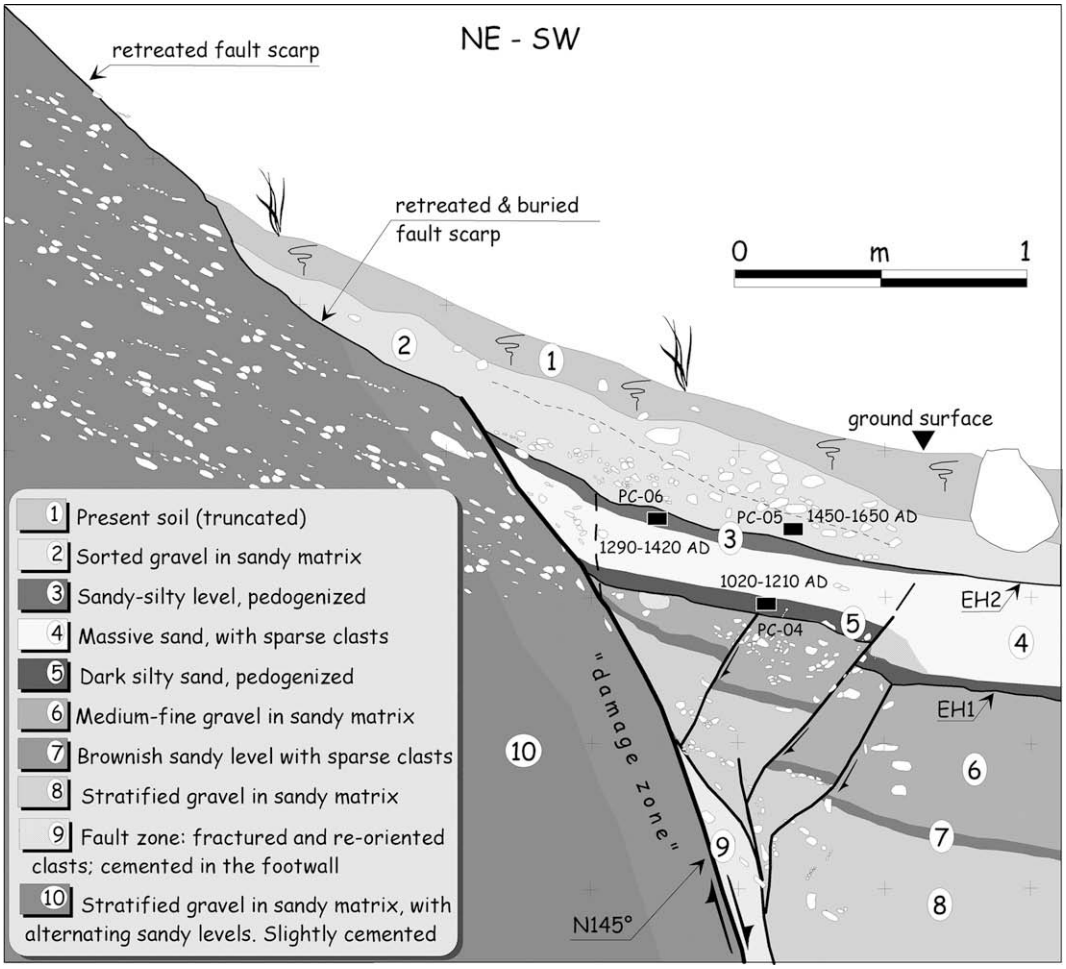

Fig. 17. Sketch of trench 1, excavated across the AIF at the foot of Mount Cesavaiutti. The last event occurred after/during the deposition/pedogenization of units 4–3, i.e., around 1290–1420 AD. A previous event occurred at EH1, a time before 1020–1210 AD. It is certain that the last rupture matches exactly with the 1349 earthquake.

the previous ruptures. As with trench 1, the last event occurred during the Low-Middle Age (time from sample PC-01, in unit 3: 1150–1270 AD), and it was sealed by units containing modern tiles, whereas the penultimate event (and a previous one?) occurred after the deposition of units 6–4, which is after 240–560 AD (sample PC-02 in unit 6).

6.3. Trench 3

This trench was excavated at the foot of Riparossa slope using a backhoe (Fig. 7). This is an almost flat area that is downhill of the prominent scarp that matches with the Miocene subvertical strata (limestone–marl passage). Therefore, we dug a narrow, 20-m-long trench through the presumed fault trace until we found it. Afterwards, we enlarged and deepened the trench in the fault zone, obtaining an 8-m-long, 4-m-deep exposure (Figs. 20 and 21). In contrast to trenches 1 and 2, the fault here is buried under 2.5 m of colluvial deposits, which are mainly made up of clayey material. Actually, almost all of the exposed deposits are clayey, both in the footwall and the hangingwall. This made the cleaning and the definition of the existing units very difficult, which suddenly become a hard, stiff, uniform wall. However, we succeed in identifying some definite features, such as the faulting of the argillitic bedrock (Miocene flysch: unit 9) against colluvia/alluvial deposits (units 8–5), and the presence and shape of a retreated and buried fault scarp that was carved into the argillitic unit.

Units 4 and 3 seal the faulted units, also burying the smoothed retreated fault scarp. In particular, unit 4 is a brownish, massive colluvium, with sparse carbonate clasts in a clayey–silty matrix that fill and level the step produced by the fault rupture. The texture and chaotic organization of the deposit might be related to solifluction/earth-flow processes; considering that the fault scarp is carved into clays and that it has been scarcely eroded and retreated, unit 4 probably deposited shortly after the faulting. Unit 2 is also a massive colluvial deposit, with sparse clasts that thicken in the hangingwall, definitively levelling the fault scarp and covering its distal retreated part. Given the origin of all of the deposits – the parent material of which are the closely outcropping marls and clays – and the complete lack of any datable elements (e.g., charcoal, wood, bones), we were not confident in the dating of bulk samples. However, considering the presence of terracotta fragments in units 2–1 (probably bricks and/or tiles) and assuming a quick deposition rate of the colluvial units 4–2, the faulting event can be tentatively dated to historical time.

A previous faulting event is tentatively testified by the existence of a higher (and older) trait of a retreat fault scarp (right side of Fig. 21), which is characterized by a lower dip with respect to the younger trait. Also in this trench, the lack of correlative units across the fault hampers the correct evaluation of the offset per-event. However, assuming that units 4–3 filled the step created by the last faulting, and considering the height of the retreated fault scarp, a minimum 0.9 m offset can be hypothesized.

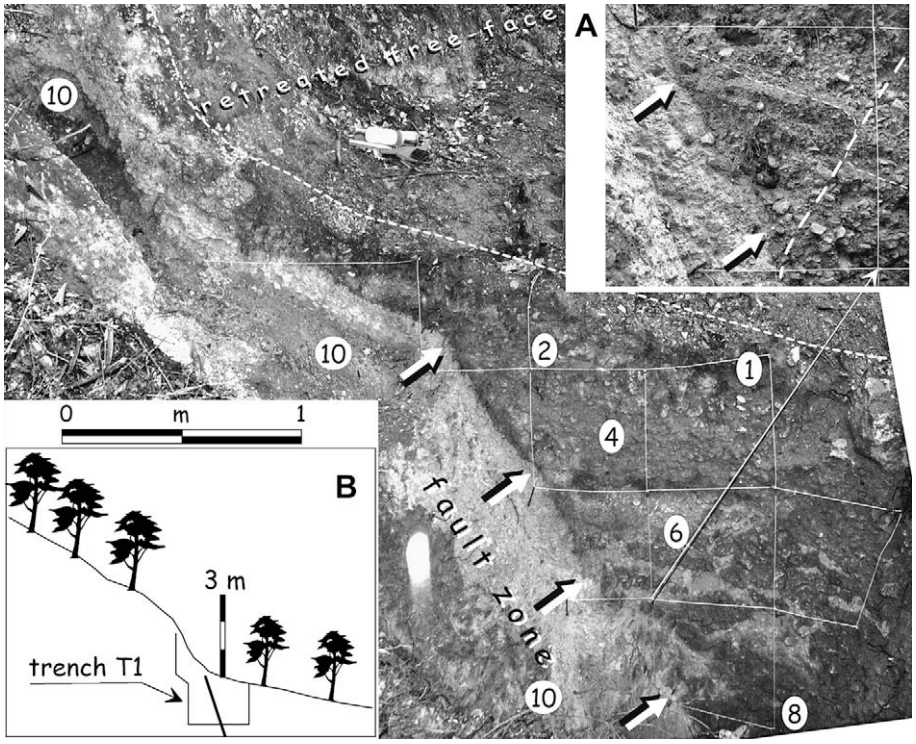

Fig. 18. Photomosaic of the SW wall of trench 1 (southern segment of the AIF; Mount Cesavaiutti hill side). Unit numbers are the same as for Fig. 17. The footwall is entirely built of post-LGM stratified slope gravels (10), which are slightly cemented near the surface. The fault zone that developed in the footwall presents an indurated fault plane. The last rupture is sealed by units 2–1. A, details of the fault zone showing a secondary splay (dashed). B, sketch of the fault scarp existing in this site, obtained by means of microtopographic surveys.

7. Archaeoseismological analyses along the Roman aqueduct of Venafro

During the field investigation along the slopes of S. Maria Oliveto–Pozzilli, we found the impressive relics of a subterranean Roman aqueduct. Thus if its track had crossed the fault trace, we would have the possibility of gathering valuable and robust information concerning the recent fault activity. The existence and path of this aqueduct have been known since Ciarlanti (1644) and Cotugno (1824), although the only reliable technical survey was carried out in the 1930s (see Frediani, 1938). The aqueduct starts from the spring of the Volturno River (548 m a.s.l.) near the San Vincenzo a Volturno Abbey, and then runs along a 31-km-long winding track until it arrives at Venafro (225 m a.s.l.). It mainly runs through a tunnel (*specus*; see Fig. 22) inside the carbonate and marly hill slopes, overtaking the *talweg* of streams by arched bridges, most of which have now collapsed. In the flat areas where the subsoil is made up of alluvial/colluvial or clayey deposits, the Romans built it into a trench and then covered the excavation. The aqueduct is known worldwide mostly for its *Tabula Aquaria* (dated from 17 to 11 BC: CIL 10, 4842; see Mommsen, 1883), an edict of the Emperor Caesar Augustus that regulated the use, restoration and maintenance of the aqueduct and of its imperial waters (Aquae Iuliae).

The *specus* is 0.6 m wide and 1.6 m high, with a round stone arch and an external structure in *opus incertum* (irregular stone masonry). The internal walls are coated with hydraulic plaster (i.e., *opus signinum* = *cocciopesto* mortar), whereas the bottom is lined with *bipedali* (i.e., typical Roman 61 × 58 cm bricks). The aqueduct was built in the first half of the 1st century AD, as has been deduced from a letter of M. Tullius Cicero (106 to 42 BC; see Cicero 1st. century BC) to his brother (*Ad Quintum fratrem*, 3, 1), and it was then finished or restored by Emperor Augustus at the end of the same century. Conversely, we do not known when it ceased to function, although it is reasonable to believe that it fell into disuse during the fall of the Roman Empire (4th–5th century) due to the lack of maintenance or due to a traumatic event. Near Pozzilli, we attempted to date the first mud layer filling the bottom of the tunnel, but we obtained an absolute age (780–410 BC 2σ calibrated age), which is not consistent with the history of the aqueduct, and it probably belonged to the parent material of the deposit that penetrated inside the *specus*.

Unfortunately, for the investigated area, neither the survey quoted by Frediani (1938) or other studies contain analytical information concerning the location and elevation of the aqueduct. Therefore, in association with the Archaeological Superintendence of Molise, we carried out a specific survey that was aimed at

Table 5
^{14}C ages of samples collected in the trenches dug across the AIF. R, standard radiometric; BLC, bulk low carbon; AMS, accelerator mass spectrometry (Beta Analytic Inc. laboratory, Miami, Florida).

Trench	Sample	Analysis	Dated material	Measured radiocarbon age	Intercept of R.A. with calib. curve	Calendric Age range sample analysis dated (2σ–95%)
T1	PC-04	AMS	Organic silt	920 ± 40 BP	1060/1080/1150 AD	1020–1210 AD
	PC-05	AMS	Organic silt	350 ± 40 BP	1500/1600/1610 AD	1450–1650 AD
	PC-06	AMS	Organic silt	610 ± 40 BP	1320/1350/1390 AD	1290–1420 AD
T2	PC-01	AMS	Organic silt	820 ± 40 BP	1210 AD	1150–1270 AD
	PC-02	R, BLC	Organic silt	1650 ± 70 BP	410 AD	240–560 AD

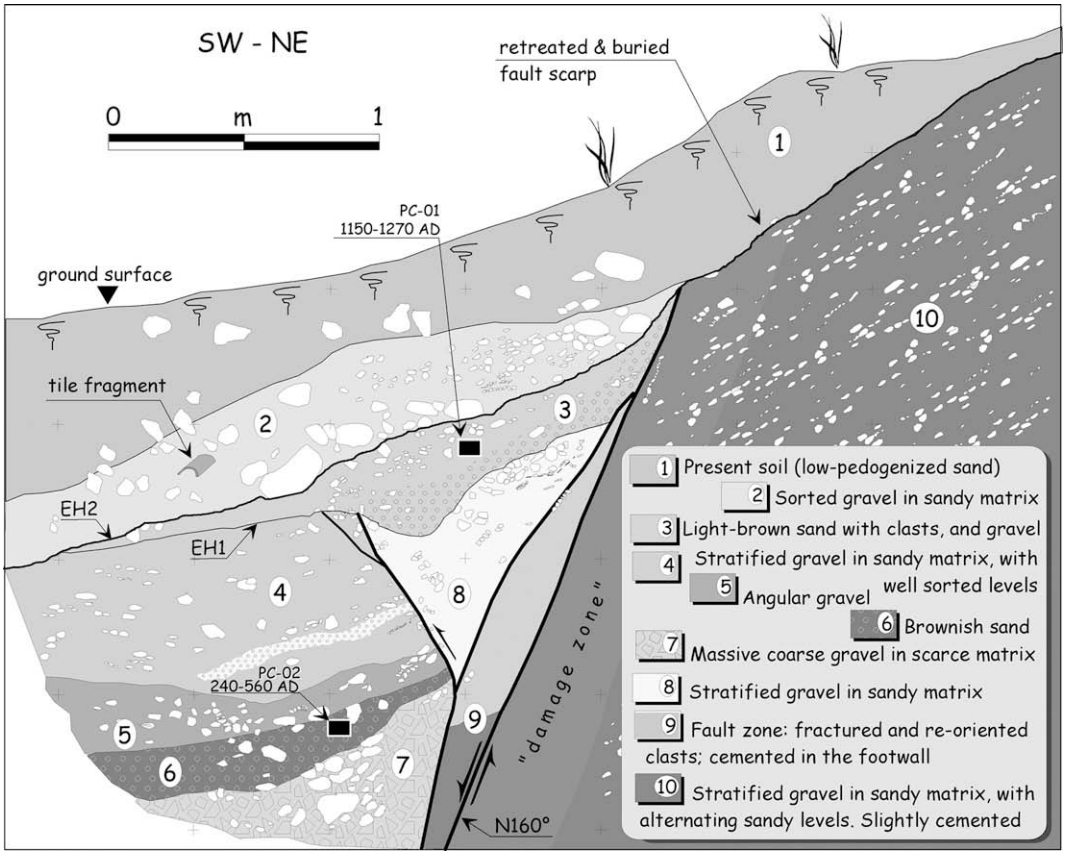

Fig. 19. Sketch of the second trench excavated across the AIF, at the foothill of Mount Cesavaiutti. The last event occurred after 1150 to 1270 AD, whereas a previous one (or more than one) occurred some time after 240 to 560 AD. Also in this case, the age of the last rupture matches with the 1349 earthquake.

discovering and measuring aqueduct relics between the villages of S. Maria Oliveto and Venafro (i.e., across the fault zone; Fig. 23). Due also to information obtained from the people of the area, we found aqueduct relics in a dozen different localities, nine of which have been directly inspected. The elevation of each point (generally the level of the *bipedali*, or the inner arch) was then measured by means of topographic levellings (associated error ± 10 cm), and positioned on 1:5,000 maps. We finally traced the path of the aqueduct by following the altimetric gradient between each observed point, obtaining a detailed map from which we have derived an actual topographic section along the 8500 m of the investigated track.

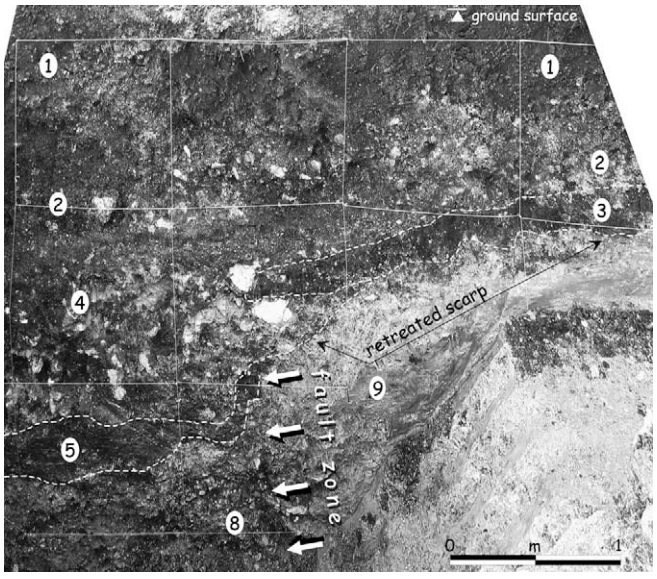

Fig. 20. Photomosaic of the NE wall of trench 3 (northern segment of the AIF). Unit numbers are the same as for Fig. 21. Unit 4 resembles a colluvial wedge filling the last fault step. Arrows indicate the fault plane.

We focused our efforts along the fault zone, where we also carried out a geomagnetic survey using a portable caesium vapour magnetometer/gradiometer (Galli et al., 2008b); Fig. 24 shows the magnetic anomaly that was measured in the footwall, which perfectly depicts the aqueduct in depth. These results are summarized in Fig. 25, which shows the aqueduct profile from S. Maria Oliveto to Venafro. The first section, from S. Maria Oliveto to the quarry site, has a 3.5/1,000 gradient, which is lower, at 2/1000, going on towards the creek, and it reaches 1/1000 between the Arcora and Ivella sites. It then rises again, to 3.2/1000, towards the Pozzilli cemetery, and to 2/1000 towards Venafro.

For our specific aims, the most significant result relates to the net step between the last observed point at Camporelle (*bipedali* level at 244.8 m a.s.l.) and the one in Arcora (240.4 m a.s.l.), which are only ~200 m away from each other. By adopting the gradient measured between the quarry site and Camporelle (2/1000), and taking the aqueduct trace towards the Arcora site, the step between the two strands is at least 3.6 m high, and it occurs exactly in the fault zone. We must exclude errors of the Roman engineers, because this part of the aqueduct was excavated in trench and in open air. Levelling errors in Roman works are known only for very long tunnel excavated under high mountains; but also in this case, the offset is in the order of centimeteres or few decimeters. Considering also that it would have been absolutely senseless for the Romans to have intentionally lost more than 3 m of hydrallic

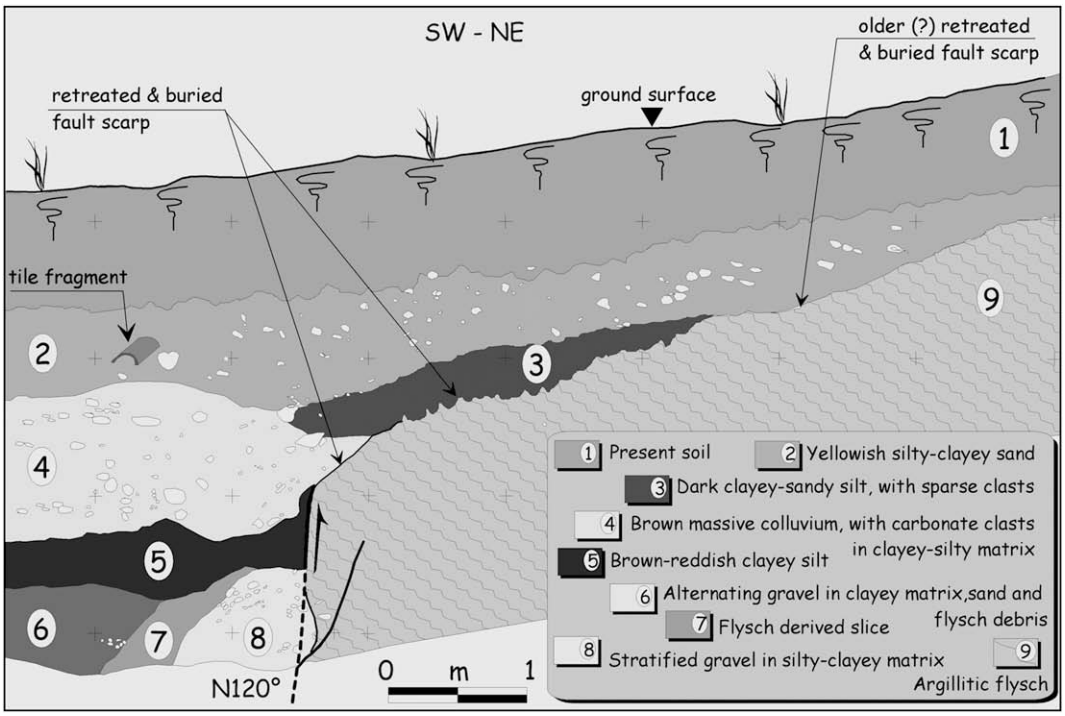

Fig. 21. Sketch of the NE wall of trench 3, excavated in the northern AlF segment (Riparossa slope). The fault separates Miocene argillitic flysch (unit 9) from chaotic clayey colluvia (8-5). A massive, mud-flow type deposit (unit 4) fills and levels the fault step, whereas units 3 and 2 seal the entire scarp. Due to the lithology and origin of the exposed materials (the argillitic formation is the proximal, parent material of all of the units), and due to the absence of any datable elements (e.g., charcoals, woods, bones), we did not feel confident enough to carry out absolute dating on any sample. The presence of sparse terracotta fragments (bricks or tiles) in units 2–1 suggests a historical time for the last burying of the fault scarp.

head before arriving at their final destination (i.e., Venafrum), and, furthermore, to have done this in a flat and clayey zone (i.e., without any morphological or lithological obstacle), we believe that this 3.6-m-high step was actually due to surface faulting.

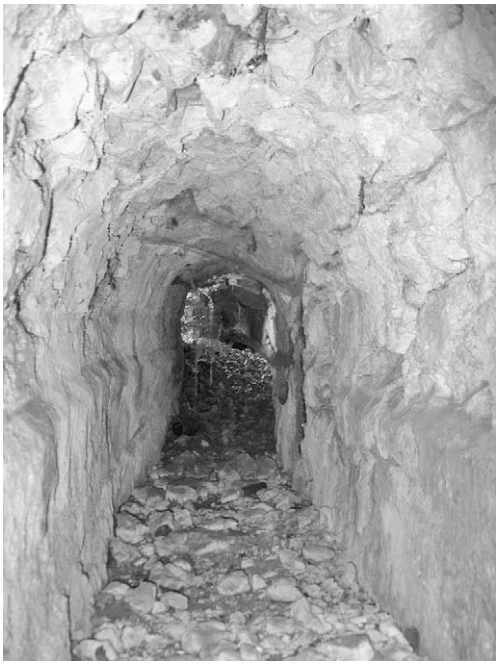

Fig. 22. Roman aqueduct. View of one tract of the tunnel that we discovered between Santa Maria Oliveto and Pozzilli. Note the ancient water level, indicated by the top of the travertine growth over the walls. Dimensions are 1.6 m (height) and 0.6 m (width). The right side and the bottom are here directly excavated in the carbonate rocks, whereas the left side and the round-arch are built with stone masonry.

Unfortunately, in this sector the aqueduct almost parallels the fault (Fig. 23), and due to the erosion of the raised block (i.e., due to fault scarp retreat processes), a dozen metres or so of its structure has been completely lost (Fig. 26). This is confirmed by the geomagnetic analyses that progressively "lose" the aqueduct traces as it neared the fault (Fig. 24). At this stage, the excavation of the aqueduct was not possible because of the presence of large olive trees.

8. Discussion and conclusions

In this study, we have applied a multidisciplinary approach with the aim of unravelling the seismotectonic context and significance of one of the largest earthquakes ever to have occurred in central-southern Italy: the September 1349 event. We focused our studies on the southern-most shock of the seismic sequence, amongst the Lazio–Molise–Campania borders.

All of the available and known historical sources were collected and re-interpreted in terms of the MCS scale, and by specifically using the intensity evaluation criteria proposed by Molin (2003). Owing also to information that was not considered previously, our data-point distribution includes 51 localities, 24 of which concern the southern-most shock, with all of these deriving exclusively from coeval sources (Table 2). On the whole, the shape of the mesoseismic area obtained strongly elongates NW–SE, between the middle Volturno Valley and the Comino Valley (Fig. 5).

Considering the geological effects that were explicitly mentioned by the historical sources (i.e., landslides), or other possible site amplification cases (i.e., villages built on thin soft alluvial sediments), the most reliable of the strongest effects of this earthquake constrain its epicentre within the Venafro area. Therefore, we focused our geological investigation on the SW Matese Massif–Venafro Mountains, where possible surface faulting had also been described by a primary, reliable source (Anonymous, 14th century). We found many indications of recent activity along

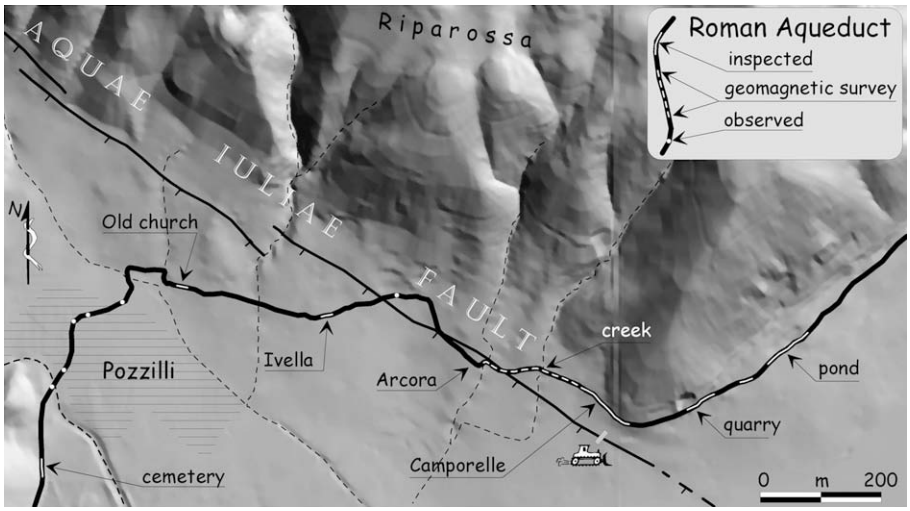

Fig. 23. Shaded relief view of the area crossed by the buried Roman aqueduct near Pozzilli (from 1:5,000 maps). Note that the aqueduct is cut by the northern segment of the Aquae Iuliae fault several times between the Ivella and creek sites. A precise topographic levelling of this tract is shown in Fig. 25. The backhoe symbol indicates the site of trench 3.

a previously poorly known NW–SE normal fault (here named the Aquae Iuliae fault; AIF) that runs for more than 20 km along the foothills of the Riparossa and Cesavaiutti–Favaracchi range, crossing the Volturno River valley, and also cutting the Imperial Roman aqueduct of Venafro (Fig. 27).

This AIF is separated into two main segments (Fig. 27) that join in the Volturno Valley. In this area, the thermal springs and travertine that have originated from deep crustal CO_2 degassing mark the linkage zone between the two segments. In the same area, the impressive flight of fluvial terraces that characterize the entire high Volturno Valley (i.e., footwall) disappears abruptly under the overflooded Venafro Plain (hangingwall; Figs. 12 and 13).

The fault location matches with our 1349 epicentral area, while its trend fits with the distribution of its effects (i.e., NW–SE). According to the empirical relationship between fault length and magnitude developed for the Apennine faults (Galli et al., 2008a), it is consistent with Mw ~6.6 earthquakes.

To provide analytical data regarding the eventual 1349 fault rupture (and/or other earthquakes), we carried out paleoseismological analyses through three trenches excavated across the AIF (Fig. 27). Following radiocarbon datings, we were able to provide some robust indications regarding the fault parameters, and in particular regarding its historical activity.

8.1. Paleoearthquakes

Leaving aside trench 3, which only provides qualitative information regarding a historical rupture of the fault, trenches 1 and 2 give robust constraints as far as the last surface faulting event is concerned. The ^{14}C dating of the units that predate the last event (unit 3 in both trenches) falls into the Low-Middle Age (samples dated from 1150 to 1270 AD, and from 1290 to 1420 AD), whereas the fault is sealed by unit 2, which is dated from 1450 to 1650 AD in trench 1, and which contains modern tile fragments in trench 2. Therefore, considering the match between the distribution of the effects and the fault trend of the 1349 earthquake, and the absolute lack – in this time interval – of any other Mw $\geq$ 6.5 earthquake (i.e., strong enough to have been generated by a capable fault; see CPTI04), we are reasonably sure that the last rupture of the AIF was related to the 9 September, 1349, earthquake.

A penultimate event is also visible in both of the trenches, before unit 3 (trench 1), and after unit 6 (trench 2), with it thus dated between 240–560 AD, and 1020–1210 AD. However, we cannot exclude the presence of more than one event in this time span, although no indications of such (e.g., colluvial wedges) are visible in either of these trenches. Robust evidence concerning repeated fault activity over the past two millennia was provided by the

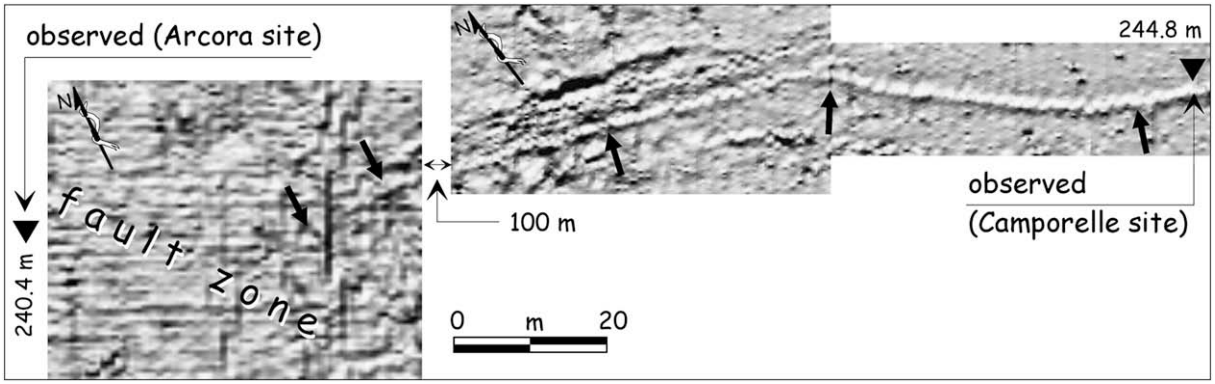

Fig. 24. Shaded relief elaboration of part of the geomagnetic survey performed along the aqueduct trace (Camporelle–Arcora tract in Figs. 23 and 25). Arrows indicate the net magnetic anomaly fitting with the aqueduct path (which, in turn, follows the local contour line). In the right panel, the *specus* is sub-outcropping (~0.5 m), whereas farther east (left panel) it disappears nearing the fault zone (i.e., it is dismantled and eroded by the progressive process of fault scarp retreating). Triangles are observed and levelled parts of the aqueduct.

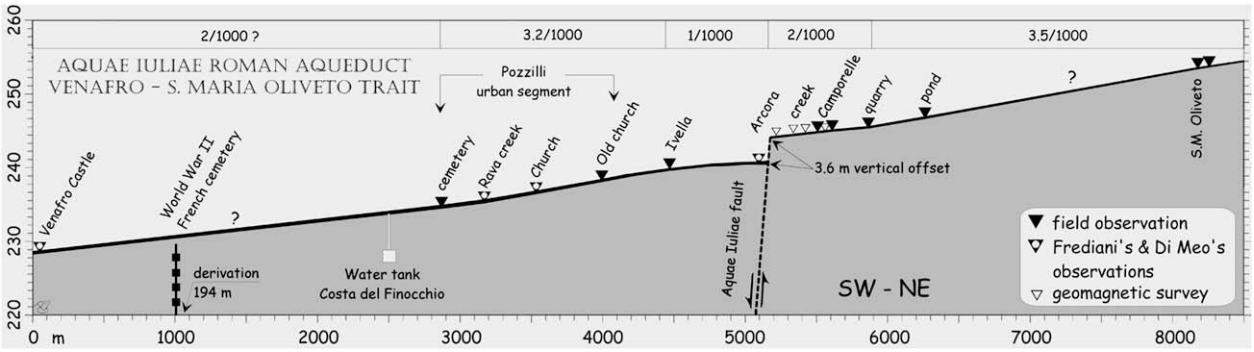

Fig. 25. Real altimetric profile of the Roman aqueduct between Venafro and S. Maria Oliveto. Note the step seen between the two strands (Venafro–Arcora *vs* Camporelle–S. Maria Oliveto), which occurs just at the fault crossing point. A continuous deformation, revealed by the lowering of the gradient, occurs as nearing the fault on both sides. For simplicity, this section does not show other possible fault/aqueduct intersections between Arcora and Ivella (e.g., in Fig. 23).

displacement of the Roman aqueduct across the northern segment of the fault, which was up to 3.6 m. If this offset is due entirely to surface faulting, as we have shown, this was obviously caused by multiple ruptures. Thus, considering the minimum offset per-event calculated in the trenches (~0.9 m), as well as the 1349 event, there should have been at least two other surface events that occurred after the design and construction of the aqueduct (1st century BC).

If we look at the known earthquakes of the area (Fig. 2), and if we consider the distribution of their effects, both the 346/355 AD and the 847 events could be reliable candidates for this faulting. In particular, most of the southern effects of the 346/355 earthquake(s) (Fig. 3) can be explained by a seismogenic source fitting with the AIF; in this case, contrary to the 1349 earthquake, we can hypothesize that the fault rupture had a SE directivity, explaining the collapse and damage in the SE quadrant of its hangingwall.

8.2. Slip rate

The most reliable short-term rate of the AIF is provided by the 3.6-m offset of the Roman aqueduct; considering that this was built ~2050 years ago, the relative net slip rate would be 1.8 mm/yr. An analogous value comes from trench 2, where a minimum value of 1.5–1.9 mm/yr can be inferred for the past 1400–1700 years.

A minimum medium-term estimate can be calculated from the Mount Cesavaiutti slope: assuming a post-LGM regularization of its profile (e.g., ~16 ka; Galli et al., 2006), the current step (plus the minimum offset of unit 10 seen in trenches 1–2) is at least 7 m, which yields a minimum slip rate of 0.45 mm/yr. On the other hand, in the fault-linkage zone, the slip rate evaluated considering the offset of the 4th order terrace's top is, instead, ~1 mm/yr.

Finally, a long-term indication can be judged by considering the terraces of the Volturno River that hang in the raised block of the fault; if we assume that the 2rd order surface, presently at ~290 m a.s.l. in the hangingwall, has more than a 120-m offset (i.e., it should be below the Volturno alluvial plain in the down-thrown block) and that it is much younger than 250 ka, the minimum slip rate for this time span would again be 0.5 mm/yr.

These values, and particularly those evaluated in the short-term, can be compared with the extension rate derived from GPS analyses (~2.7 mm/yr; Giuliani et al., in press). Taking into account that a slip rate of 1.8 mm/yr yields an extension rate of ~0.8 mm/yr on a normal fault (~65° average dip), the ongoing regional extension of the upper crust across the SW Matese Massif can be partly explained by aseismic strain, and to coseismic rupture across the AIF.

8.3. Recurrence and elapsed time

As discussed above, apart from the 1349 event, we have no definitive data as far as the age of paleoearthquakes is concerned. A hypothesis that does not claim to be conclusive is that both the 346/355 and the 847 earthquakes were generated by the AIF; in this case, we would have ~0.5 ka of return time. This value fits with an indirect estimate, i.e., by dividing the offset per-event by the slip rate of the past two millennia. On the other hand, if we consider the medium- or long-term slip rates, the recurrence time increases to ~1.5 ka; however, this must be considered a minimum value, because it is derived, in turn, from minimum slip rates. The elapsed time is, obviously, 659 years.

8.4. Concluding remarks

We can confirm that the AIF is one of the most seismically hazardous faults of the Apennine chain, as it is probably responsible for some of the most catastrophic earthquakes of Antiquity in Italy.

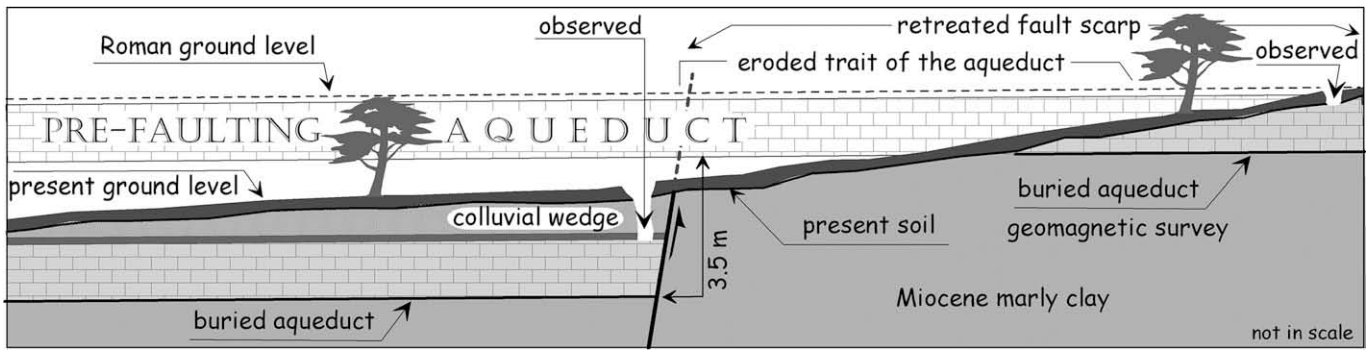

Fig. 26. Sketch of the aqueduct in the fault zone (not to scale). Relics of the aqueduct were seen and their altitude was calculated, both in the hangingwall and in the footwall (arrows). Here, the absence of the tunnel nearing the fault has been confirmed by geomagnetic analyses.

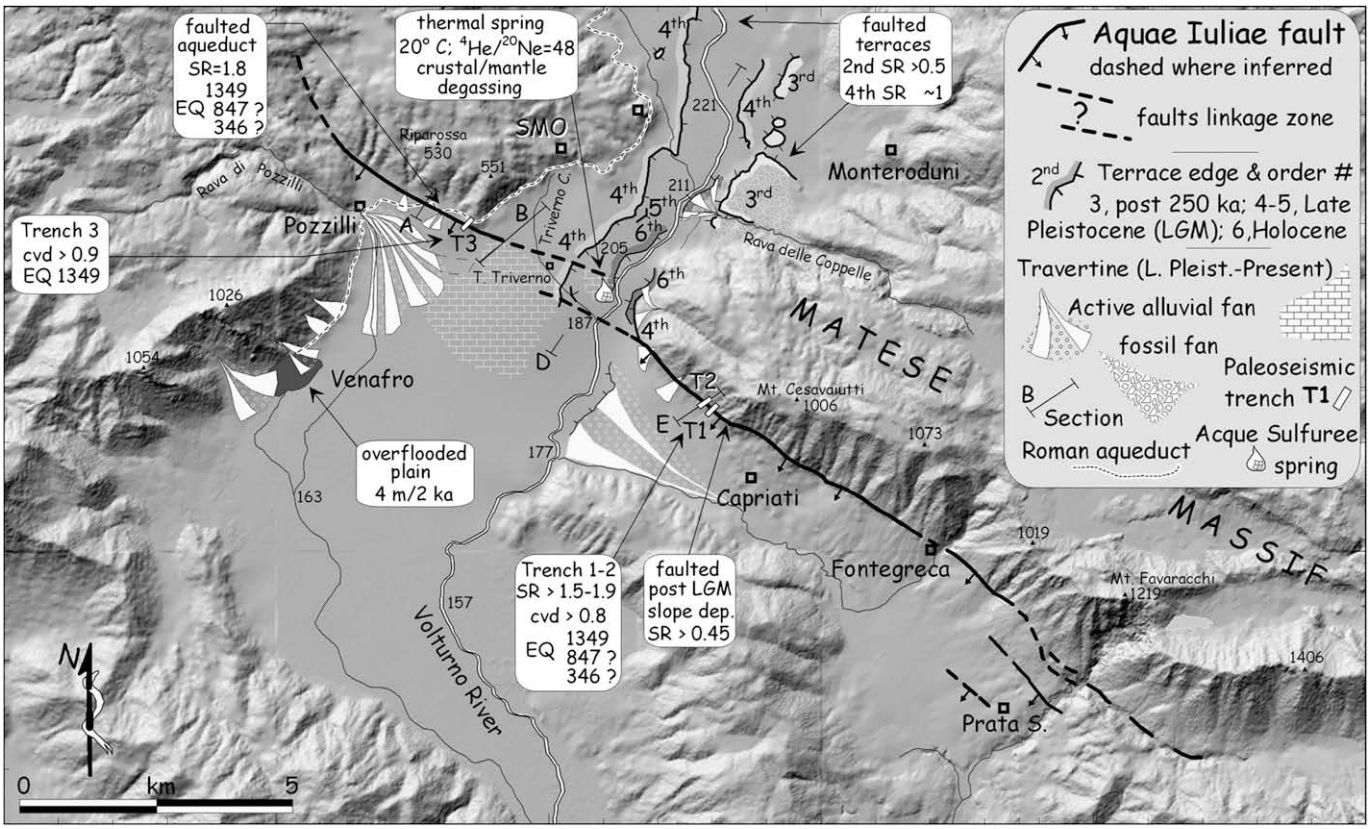

Fig. 27. Summary sketch of the main features regarding the Aquae Iuliae fault activity (shaded relief base from 1:25,000 maps). Note the terraces carved in the footwall (uplifted block), which end abruptly in the fault zone (see also Figs. 12 and 13; the 1st–2nd order terrace are out of the map area). Hydrothermal activity and travertine deposition occur at the fault tips (i.e., in the linkage zone), where the intense and continuous rock fracturing causes a breakdown region (*sensu* Scholz et al., 1993). The map also shows the location of the paleoseismological trenches and a segment of the Augustean aqueduct that was affected by the fault. Labels in panels are: SR, vertical slip rate (mm/yr); cvd, coseismic vertical displacement (m); EQ, earthquake rupture year.

Its discovery and parameterization will hopefully improve the current seismogenic zonation of Italy. From a geological point of view, it is also worth noting that the AIF represents the only seismogenic structure in Italy that crosses a major alluvial valley (i.e., Volturno River), making an impressive case of tectonics-controlled fluvial morphology.

In our hypothesis, its recurrence time is the shortest of those for the Apennines, as the slip rate is one of the highest. Together with the neighbouring northern Matese fault system, it accommodates a large amount of the NE–SW extension presently affecting this sector of the chain, as also confirmed by GPS analyses. Its univocal association with the 1349 earthquake and, reasonably, with the 346/355 and 847 events, allows to better locate the epicentres of these events, which have moved around so much in recent seismic studies (Table 1). However, we cannot exclude that the contemporary rupture of an unknown fault adjoining the AIF in the Comino Valley region (Fig. 2) might have partly contributed to the 1349 damage distribution in the area. This hypothesis is supported by the existence of the 1654 earthquake source (see the mesoseismic NW-SE elongation in Fig. 5, which depicts a possible similarly trending seismic source), which could share part of its seismogenic structure with that of 1349.

8.5. Ongoing research

In association with the Archaeological Superintendence of Molise, we have started a research project aimed at the exhumation of the Roman aqueduct in the fault zone. The results are likely to constrain the age of the faulting of this two-thousand-year-old work, prior to the 1349 event (e.g., the 346/355 and 847 events?). On the other hand, studies on the flight of fluvial terraces in the Volturno Valley – in association with CNR-IGAG of Rome – will hopefully define the incremental slip history of the fault during the Late Pleistocene, thanks also to tephrachronology analyses.

Acknowledgments

We thank: Biagio Giaccio and Paolo Messina (CNR-IGAG) for the tephra analyses and for discussing the geomorphological evolution of the area with us; Stefania Capini (Archaeological Superintendence of Molise), and Luigi Scaroina (Istituto Romano di Archeologia) for their professional and friendly archaeological support; Tonino Palazzo (Superintendence at the Antiquity of Molise) for helping us with the aqueduct survey; Eugenio di Meo (poet and peasant) who showed us all of the aqueduct strands that he had discovered; Angelo Gambella (Medioevo Italiano Project) for his useful discussions on the Middle Age topography of the investigated area; Giovanni Salvietti (ENEL) for the archive research in Naples; Claudio Carrara (AIQUA) for discussing the travertine origin with us; Jan Sevink (University of Amsterdam) for all of the material he provided us with and for the useful discussions on the Quaternary evolution of the area; Alessandro Giocoli, Sabatino Piscitelli and Enzo Rizzo (CNR-IMAA, Potenza) for the geophysical analyses carried out along the aqueduct and across the travertine; Salomon Hailemikael (University of Rome) for helping us during the geological survey and with the digging of the pits; Paolo Passarelli (Municipality of Pozzilli) for the logistic support during the trenching work; and Piero de Pari (Geoservizi s.r.l., Campobasso) for providing us with so much of the geological information of the subsoil.

The views and conclusions contained in this paper are those of the authors and should not be interpreted as necessarily representing official policies, either expressed or implied, of the Italian Government.

References

Altunen, E., Hancock, P.L., 1993. Morphological features and tectonic setting of Quaternary travertines at Pamukkale, western Turkey. Geological Journal 28, 335–346.

Anderson, H., Jakson, J., 1987. Active tectonics of the Adriatic Region. Geophysical Journal of the Royal Astronomic Society 91, 937–983.

Anonymous, 14th century. 1349 Parchment, in Archivio del Capitolo Cattedrale di Isernia, Pergamene, FASC. V, 7.

Anonymus Monachus Casinensis, 13th–14th century. Rerum in regno Neapolitano gestarum breve chronicon. In: L.A. Muratori (Ed.), Rerum Italicarum Scriptores, vol. 5, 55–78.

Baratta, M., 1901. I terremoti d'Italia, Saggio di storia, geografia e bibliografia sismica italiana. Fratelli Bocca Editori, Torino, 950 pp.

Berardi, R., Contri, P., Galli, P., Mendez, A., Pacor, F., 1999. Modellazione degli effetti di amplificazione locale nelle città di Avezzano, Ortucchio e Sora. In: Castenetto, S., Galadini, F. (Eds.), 13 gennaio del 1915. Il terremoto nella Marsica. Servizio Sismico Nazionale, pp. 349–372.

Blumetti, A.M., Caciagli, M., Di Bucci, D., Guerrieri, L., Michetti, A.M., Naso, G., 2000. Evidenze di fagliazione superficiale olocenica nel bacino di Boiano (Molise). Extended abstracts of the 19° GNGTS congress, Rome 7–9 November, Cd-rom, ISBN: 88-900-385-4-3, 9 pp.

Bonito, M., 1691. Terra tremante, o vero continuatione de li tremuoti dalla Creatione del mondo sino al tempo presente. Parrino & Muti, Napoli, 822 pp.

Boschi, E., Ferrari, G., Gasperini, P., Guidoboni, E., Smriglio, G., Valensise, G. (Eds.), 1995. Catalogo dei forti terremoti in Italia dal 461 a.C. al 1980. ING-SGA, Bologna, 970 pp.

Boschi, E., Guidoboni, E., Ferrari, G., Valensise, G., Gasperini, P. (Eds.), 1997. Catalogo dei forti terremoti in Italia dal 461 a.C. al 1990. ING-SGA, Bologna, 644 pp.

Boschi, E., Guidoboni, E., Ferrari, G., Mariotti, D., Valensise, G., Gasperini, P. (Eds.), 2000. Catalogue of Strong Italian Earthquakes from 461 B.C. to 1997. Version 3 of the Catalogo dei forti terremoti in Italia. Annals of Geophysics, vol. 43, pp. 609–868.

Bosi, V., 1994. Evoluzione tettonica del Lazio meridionale e della Campania settentrionale in corrispondenza della terminazione della linea tettonica "Ortona-Roccamonfina". Ph.D. thesis. University of Rome.

Brancaccio, L., Cinque, A., Di Crescenzo, G., Santangelo, N., Scarciglia, F., 1997. Alcune osservazioni sulla tettonica quaternaria nell'Alta Valle del F. Volturno. Il Quaternario 10, 321–328.

Brancaccio, L., Di Crescenzo, G., Rosskopf, C., Santangelo, N., Scarciglia, F., 2000. Carta geologica dei depositi quaternari e Carta geomorfologica dell'Alta Valle del Volturno (Molise, Italia meridionale). Note illustrative. Il Quaternario 13, 81–94.

Caiazzo, C., Ruggieri, G., Morra, V., Santangelo, N., Villa, I., 2001. Quaternary evolution of Prata Sannita Basin (Southern Italy). Morphostructural, microtectonic and radiometric analysis. Workshop "Uplift and erosion: driving processes and resulting landform". Certosa di Pontignano (Si), September 20–21 2001. (abstracts).

Çakir, Z., 1999. Along-strike discontinuity of active normal faults and its influence on quaternari travertine deposition; example from western Turkey. Turkish Journal of Earth Science 8, 67–80.

Camassi, R., Stucchi, M., 1996. NT4.1, un catalogo parametrico di terremoti di area italiana al di sopra della soglia del danno. GNDT, Milan, 66 pp.

Castello, B., Selvaggi, G., Chiarabba, C., Amato, A., 2006. CSI Catalogo della sismicità italiana 1981–2002, version 1.1. Available from:. INGV-CNT, Roma http://www.ingv.it/CSI/.

Capini, S., Galli, P., 2003. I terremoti in Molise. In: De Benedittis, R., Di Niro, A., Di Tommaso, D., Muccilli, O. (Eds.), Dal 280 A.C. al 31 ottobre 2002 – I terremoti in Molise, Guida alla mostra. Ministero per i Beni e le Attività Culturali, Campobasso, 47 pp.

Chronica Monasterii Casinensis, 12th century. 1980. In: Monumenta Germaniae Historica, Scriptores, 34, Hannover, 773 pp.

Chronica Sancti Benedicti Casinensis, 9th century. In: Waitz, G. (Ed.), Monumenta Germaniae Historica, Scriptores rerum Langobardicarum et Italicarum saec, vol. VI–IX, Hannover, 649 pp.

Chronicon breve Atinensis ecclesia, 14th century. In: L.A. Muratori (Ed.), Rerum Italicarum Scriptores, vol. 7, 901–912.

Ciarlanti, G.V., 1644. Memorie historiche del Sannio chiamato hoggi Principato Ultra, contado di Molisi e parte di terra di lavoro, provincie del Regno di Napoli, Isernia, 530 pp.

Cicero, M.T., 1989. 1st century BC. Epistulae ad Quintum fratem. In: Salvatore, A. (Ed.). Mondadori, Milano, 126 pp.

Cinque, A., Ascione, A., Caiazzo, C., 2000. Distribuzione spazio-temporale e caratterizzazione della fogliazione quaternaria in Appennino meridionale. In: Galadini, F., Meletti, C., Rebez, A. (Eds.), Le ricerche del GNDT nel campo della pericolosità sismica (1996–1999). CNR-GNDT, Roma, pp. 203–218.

Cinque, A., Patacca, E., Scandone, P., Tozzi, M., 1993. Quaternary kinematic evolution of the Southern Apennenes. Relationships between surface geological features and deep lithospheric structures. Annali di Geofisica 36, 249–260.

Coltorti, M., Cremaschi, M., 1981. Depositi quaternari e movimenti tettonici nella conca di Isernia. C.N.R., P.F.G., Sottoprogetto neotettonica. Contributi conclusivi per la realizzazione della Carta Neotettonica d'Italia, Pubbl. 506, pp. 173–188.

Coltorti, M., 1983. Le fasi principali dell'evoluzione di paesaggio nel bacino di Isernia (Molise). Isernia La Pineta. Calderini, Bologna, pp. 41–49

Corniello, A., Ducci, D., Guarino, P.M., 1999. I rilievi carbonatici del Matese occidentale e la piana di Venafro: idrogeologia e idrogeochimica. Bollettino Società Geologica Italiana 118, 523–535.

Cotugno, G., 1824. Memorie istoriche di Venafro, Napoli, 348 pp.

Cronicon siculum, 14th century. In: De Blasis, J. (Ed.), Cronicon siculum incerti authoris ab anno 340 ad annum 1396 in forma diary ex inedito Codice Ottoboniano Vaticano, Napoli, 143 pp.

Curewitz, D., Karson, J.A., 1997. Structural setting of hydrothermal outflow: fracture permeability maintained by fault propagation and interaction. Journal of Volcanology and Geothermal Research 79, 149–168.

D'Agostino, N., Jackson, J.A., Dramis, F., Funiciello, R., 2001. Interactions between mantle upwelling, drainage evolution and active normal faulting: an example from the Central Apennines (Italy). Geophysical Journal International 147, 475–497.

Deino, A.L., Orsi, G., de Vita, S., Piochi, M., 2004. The age of the Neapolitan Yellow Tuff caldera-forming eruption (Campi Flegrei caldera – Italy) assessed by $^{40}Ar/^{39}Ar$ dating method. Journal of Volcanology and Geothermal Research 133, 157–170.

De Mets, C., Gordon, R.G., Argus, D.F., Stein, S., 1990. Current plate motions. Geophysical Journal International 101, 425–478.

Di Bucci, D., Corrado, S., Naso, G., Villa, I., 2005. Growth, interaction and seismogenic potential of coupled active normal faults (Isernia Basin, central-southern Italy). Terra Nova 17, 44–55.

Doglioni, C., 1991. A proposal for the kinematic modelling of W dipping subductions: possible applications to the Tyrrhenian–Apennines system. Terra Nova 3, 423–434.

Doglioni, C., Mongelli, F., Pieri, P., 1994. The Puglia uplift (SE Italy): an anomaly in the foreland of the Apenninic subduction due to buckling of a thick continental lithosphere. Tectonics 13, 1309–1321.

Dramis, F., 1983. Morfogenesi di versante nel Pleistocene superiore in Italia: i depositi detritici stratificati. Geografia Fisica e Dinamica del Quaternario 6, 180–182.

Enel-Ismes, 1986. I terremoti del settembre 1349. Studi ed indagini per l'accertamento della idoneità tecnica delle aree suscettibili di insediamento di impianti nucleari, Regione Puglia aerea costiera salentina adriatica, Indagini di sismicità storica, Rapporto finale, RAT-DGF-0001, 391 pp.

Figliuolo, B., Marturano, A., 2002. Terremoti in Italia meridionale dal IX all'XI secolo. In: Marturano, A. (Ed.), Contributi per la storia dei terremoti nel bacino del Mediterraneo (secc. V-XVIII). Salerno, pp. 33–67. Laveglia.

Frediani, F., 1938. L'acquedotto augusteo di Venafro. Riassunto e rilievi a cura dell'Ente Volturno. Istituto di Studi Romani, Campania Romana, Studi e Materiali. Rispoli Anonima Editore, Napoli, pp. 163–185.

Galadini, F., Galli, P., 2000. Active tectonics in the central Apennines (Italy) – input data for seismic hazard assessment. Natural Hazards 22, 202–223.

Galadini, F., Galli, P., 2004. The 346 A.D. earthquake (central-southern Italy): an archaeoseismological approach. Annals of Geophysics 47, 885–905.

Galli, P., Galadini, F., 2003. Disruptive earthquakes revealed by faulted archaeological relics in Samnium (Molise, southern Italy). Geophysical Research Letters 30, 1266, doi:10.1029/2002GL016456.

Galli, P., Naso, G., 2008. The "taranta" effect of the 1743 earthquake in Salento (Apulia, southern Italy). Bollettino di Geofisica Teorica ed Applicata 49, 177–204.

Galli, P., Bosi, V., Piscitelli, S., Giocoli, A., Scionti, V., 2006. Late Holocene earthquakes in southern Apennines: paleoseismology of the Caggiano fault. International Journal of Earth Sciences 95, 855–870.

Galli, P., Galadini, F., Pantosti, D., 2008a. Twenty years of paleoseismology in Italy. Earth Science Review 88, 89–117, doi:10.1016/j.earscirev.2008.01.001.

Galli, P., Naso, G., Capini, S., Giocoli, A., Hailemikael, S., Piscitelli, S., Rizzo, E., Scaroina L., 2008b. Faulting of the Roman aqueduct of Venafrum (Italy); investigation methodology and preliminary results, 31st General Assembly of the European Seismological Commission ESC 2008, Hersonissos, Crete, Greece, 7–12 September 2008, Short Papers volume, 94–100.

Galli, P., Giaccio, B., Messina, P., Naso, G., 2008c. L'influenza della tettonica attiva nello sviluppo di terrazzi alluvionali: il caso della faglia delle Aquae Iuliae nella media valle del Volturno (Venafro, appennino centro-meridionale), Extended abstracts of the 27° GNGTS Congress, Trieste 6–8 October 2008, 150–154.

Gasperini, P., 2002. The Boxer program, release 3.02. Available from: http://ibogfs.df.unibo.it/user2/paolo/www/boxer/boxer.html.

Giannetti, B., De Casa, G., 2000. Stratigraphy, chronology, and sedimentology of ignimbrites from the white trachytic tuff, Roccamonfina Volcano, Italy. Journal of Volcanology and Geothermal Research 96, 243–295.

Giuliani, R., D'Agostino, N., D'Anastasio, E., Mattone, M., Bonci, L., Calcaterra, S., Gambino, P. Merli, K. Active extension and strain accumulation in the Molise region (Southern Apennines, Central Italy). Bollettino di Geofisica Teorica ed Applicata, in press.

Guidoboni, E., Comastri, A., Traina, G., 1994. Catalogue of ancient earthquakes in the Mediterranean area up to 10th century. ING-SGA, Bologna, 504 pp.

Guidoboni, E., Comastri, A., 2005. Catalogue of earthquakes and tsunamis in the Mediterranean area from the 11th to the 15th century, Istituto Nazionale di Geofisica e Vulcanologia, Rome-Bologna, 1037 pp.

Guidoboni, E., Ferrari, G., Mariotti, D., Comastri, A., Tarabusi, G., Valensise, G., 2007. CFTI4Med, Catalogue of Strong Earthquakes in Italy (461 B.C.-1997) and Mediterranean Area (760 B.C.-1500). http://storing.ingv.it/cfti4med/.

Hancock, P.L., Chalmers, R.M.L., Altunel, E., Çakir, Z., Becher-Hancock, A., 2000. Creation and destruction of travertine monumental stone by earthquake faulting at Hierapolis, Turkey. In: Geological Society, London, Special Publications, vol. 171, doi:10.1144/GSL.SP.2000.171.01.02, pp. 1–14.

Iohanna Duracii, 1370. Privilege of the Queen of Naples Joanna I of Anjou, In: De Utris C., 19° cent. Annali di Venafro, L. VI, pp. 12–16.

Jerome, 22–23 March 2002. 4th century. Chronicle. In: Benoit, J., Lancon, B. (Eds.), Saint Jerome, Chronique: continuation de la Chronique d'Eusebe annees 326–378. Actes de la table ronde du GESTIAT, Brest, Rennes, 207 pp.

Ladyslaus Duracii, 1401. Privilege of the King of Naples Ladilsaus of Anjou, In: De Utris C., 19° cent. Annali di Venafro, L. VI, pp. 65–69.

Lermo, J., Chavez-Garcia, F.J., 1994. Are microtremors useful in site response evaluation? Bullettin of the Seismological Society of America 84, 1350–1364.

Duchense, L. (Ed.), 1886–1957, Liber Pontificalis, 9th–15th century 3 voll., Paris.

Magri, G., Molin, D., 1984. Il terremoto del dicembre 1456 nell'Appennino centro-meridionale. Comitato Nazionale Energia Nucleare, CNEN, Rome, 180 pp.

Malinverno, A., Ryan, W.B.F., 1986. Extension in the Tyrrhenian sea and shortening in the Apennines as result of arc migration driven by sinking of the lithosphere. Tectonics 5, 227–245.

Manetti, G., 1457. In: Molin, D., Scopelliti, C. (Eds.), De Terraemotu Libri tres, collana commissione ENEA/ENEL per lo studio dei problemi sismici connessi con la realizzazione di impianti nucleari. Romana Editrice, Roma, 1983, 152 pp.

Mantenuto, S., Bonci, L., Calcaterra, S., D'Agostino, N., Giuliani, R., Mattone, M., Merli, K., 2007. Analysis of active extension in the Central Apennines (Abruzzo, Italy) using GPS measurements. Geophysical Research Abstracts 9, 04341. EGU2007-A-04341.

Mantenuto, S., D'Agostino N., 2007. Analysis of the active extension in the northern Apennines (Umbria-Marche, Italy) using CGPS measurements. Extended abstracts of the 26° GNGTS Congress, Rome 13–15 November 2007, pp. 100–101.

Maria Duracii, 1358. Privilege of Mary of Anjou, in De Utris C., 19° cent. Annali di Venafro, L. VI, pp. 1–5.

MedNet, 2008. Mediterranean Very Broadband Seismograghic Network. Available from: http://mednet.rm.ingv.it/ (accessed February 2008).

Meletti, C., Patacca, E., Scandone, P., Figliuolo B., 1988. Il terremoto del 1456 e la sua interpretazione nel quadro sismotettonico dell'Appennino meridionale, In: Figliuolo B.: Il terremoto del 1456, Edizioni Studi Storici Meridionali, Altavilla Silentina (SA), 1, 70–108; 2, 35–163.

Molin, D., 1995. Indagini Macrosismiche. In: Carrara, C. (Ed.), Lazio Meridionale, Sintesi delle ricerche geologiche multidisciplinari. ENEA, Serie Studi e Ricerche, Roma 193–222; 325–350.

Molin, D., 2003. Considerazioni sull'eventuale adozione in Italia della recente scala macrosismica europea (EMS-1998). Extended abstracts of the 22° GNGTS Congress, Rome, 18–22 November, Cd-rom ISBN/ISSN: 88-900385-9-4, 06.21, 11 pp.

Molin, D., Galadini, F., Galli, P., Mucci, L., Rossi, A., 1999. Terremoto del Fucino del 13 gennaio 1915. Studio macrosismico. In: Castenetto, S., Galadini, F. (Eds.), 13 gennaio del 1915. Il terremoto nella Marsica. Servizio Sismico Nazionale, pp. 321–340.

Mommsen, T. (Ed.), 1883. Inscriptiones Bruttiorum, Lucaniae, Campaniae, Siciliae, Sardiniae Latinae. G. Reimerum, Berlin, 1229 pp.

Montone, P., Mariucci, M.T., Pondrelli, S., Amato, A., 2004. An improved stress map for Italy and surrounding regions (central Mediterranean). Journal of Geophysical Research 109, doi:10.1029/2003JB002703.

Notar Santo di Venafro, 1423. Notarial deed transcribed by L. Valla, Storia di Venafro, manuscript dated 1692, c/o Del Prete Family, Venafro.

Orsi, G., D'Antonio, M., de Vita, S., Gallo, G., 1992. The Neapolitan Yellow Tuff, a large-magnitude trachytic phreatoplinian eruption: eruptive dynamics, magma withdrawal and caldera collapse. Journal of Volcanology and Geothermal Research 5, 275–287.

Otterloo van, R.H., 1981. Soil and landascape genesis of the Upper Volturno basin. Unpublished Ph.D. thesis. Amsterdam.

Otterloo van, R.H., Sevink, J., 1983. The quaternary evolution of the Upper-Volturno basin, in Isernia La Pineta – Un accampamento più antico di 700.000 anni, Calderini, pp. 35–39.

Pacca, N.A., 16th century. Discorso del terremoto, MS 7/A3. Società Napoletana di Storia Patria, Fondo sismico, Napoli, Italy.

Pace, B., Boncio, P., Lavecchia, G., 2002. The 1984 Abruzzo earthquake (Italy): an example of seismogenic process controlled by interaction between differently oriented synkinematic faults. Tectonophysics 350, 237–254.

Pantosti, D., Schwartz, D.P., Valensise, G., 1993. Paleoseismology along the 1980 surface rupture of the Irpinia fault. Implications for earthquake recurrence in the Southern Apennines, Italy. Journal Geophysical Research 98, 6561–6577.

Patacca, E., Sartori, R., Scandone, P., 1990. Tyrrhenian basin and Apenninic arcs: kinematic relations since Late Tortonian times. Memorie Società Geologica Italiana 45, 425–451.

Patacca, E., Scandone, P., 1989. Post-Tortonian mountain building in the Apennines: the role of the passive sinking of a relic lithospheric slab. In: Boriani, A., Bonafede, M., Piccardo, G.B., Vai, G.B. (Eds.), The Lithosphere in Italy: Advance in Earth Science Research. Accademia Nazionale dei Lincei, Rome, pp. 157–176.

Patacca, E., Scandone, P., 2007. Geology of the Southern Apennines. Bollettino Società Geologica Italiana 7, 75–119 (Special Issue).

Paternoster, M., 1999. Caratterizzazione geochimica di fluidi dell'Appennino meridionale. Univ. degli Studi della Basilicata. Unpublished post-graduate thesis.

Petrarch, F., 1350. Letter to Luigi Santo di Campinia (ad Socratem suum). In: Francesco Petrarca, Opere: Familiarum Rerum Libri, XI, vol. 7, Sansoni, Florence, 1383 pp.

Petrarch, F., 1353. Letter to Angelo di Pietro Stefano dei Tosetti (ad Lelium suum). In: Francesco Petrarca, Opere: Familiarum Rerum Libri, XV, vol. 9, Sansoni, Florence, 1383 pp.

Pliny the Elder, 1st century. In: Giardini, D. (Ed.), Naturalis Historia, vol, 5, Pisa, 1336 pp.

Polani, N., 1459. Roma Gerusalemme Celeste, Agostino, Civitas Dei, Bibliothéque Sainte Geneviéve, ms. lat. 218, f2r, Paris.

Pondrelli, S., Salimbeni, S., Ekström, G., Morelli, A., Gasperini, P., Vannucci, A., 2006. The Italian CMT dataset from 1977 to the present. Physics of the Earth and Planetary International 159, 286–303, doi:10.1016/j.pepi.2006.07.008.

Postpischl, D., 1985. Catalogo dei terremoti italiani dall'anno 1000 al 1980. Quaderni della Ricerca Scientifica 114 (2B), 239.

Prudenzio, G., 1574. Discrittione d'Alvito et suo contado, manuscript In: Santoro D., Pagine sparse di storia alvitana, 1908, 226–257.

Royden, L., Patacca, E., Scandone, P., 1987. Segmentation and configuration of subducted lithosphere in Italy: an important control on thrust-belt and foredeep-basin evolution. Geology 15, 714–717.

Scholz, C.H., Dawers, N.H., Yu, J.Z., Anders, M.H., Cowie, P.A., 1993. Fault growth and fault scaling laws: preliminary results. Journal of Geophysical Research 98, 21951–21961.

Serpelloni, E., Anzidei, M., Baldi, P., Casula, G., Galvani, G., 2005. Crustal velocity and strain-rate fields in Italy and surrounding regions: new results from the analysis of permanent and non-permanent GPS networks. Geophysical Journal International 161, 861–880.

Serpelloni, E., Casula, G., Galvan, A., Anzidei, M., Baldi, P., 2006. Data analysis of permanent GPS networks in Italy and surrounding regions: application of a distributed processing approach. Annals of Geophysics 49, 1073–1104.

SGN, Servizio Geologico Nazionale, 1971. Note illustrative alla Carta Geologica d'Italia, Foglio 161 "Isernia".

Symmacus, 1972. 4th century. [Quintus Aurelius] Epistulae, Livres 1.-2. In: Callu, J.P. (Ed.), Les belles Lettres, Paris, 238 pp.

Tertulliani, A., 2000. Qualitative effects of local geology on damage pattern. Bullettin Seismological Society of America 90, 1543–1548, doi:10.1785/0120000038.

Villani, M., 14th century. Cronica, con la continuazione di Filippo Villani. Porta G., Parma, vol. 1(1), 86–87.

Ward, S., 1994. Constraints on the seismotectonics of the central Mediterranean from very long baseline interferometry. Geophysical Journal International 117, 441–452.

Westaway, R., Gawthorpe, R., Tozzi, M., 1989. Seismological and field observations of the 1984 Lazio–Abruzzo earthquakes: implications for the active tectonics of Italy. Geophysical Journal of the Royal Astronomical Society 98, 489–514.

Working Group, 2004. CPTI Catalogo Parametrico dei Terremoti Italiani (versione 2004, CPTI04). http://emidius.mi.ingv.it/CPTI/ Internet website INGV Sezione di Milano(accessed 27.05.04).

Wulf, S., Kraml, M., Brauer, A., Keller, J., Negendank, J.F.W., 2004. Tephrochronology of the 100 ka lacustrine sediment record of Lago Grande di Monticchio (southern Italy). Quaternary International 122, 7–30.